JOURNAL OF NATURAL PRODUCTS

Article

Cite This: J. Nat. Prod. XXXX, XXX, XXX−XXX

pubs.acs.org/jnp

Isolation, Derivative Synthesis, and Structure−Activity Relationships of Antiparasitic Bromopyrrole Alkaloids from the Marine Sponge *Tedania brasiliensis*

Lizbeth L. L. Parra,[†,‡,#] Ariane F. Bertonha,[†,§,#] Ivan R. M. Severo,[†] Anna C. C. Aguiar,[⊥] Guilherme E. de Souza,[⊥] Glaucius Oliva,[⊥] Rafael V. C. Guido,[⊥] Nathalia Grazzia,[∥] Tábata R. Costa,[∥] Danilo C. Miguel,[∥] Fernanda R. Gadelha,[∥] Antonio G. Ferreira,[▽] Eduardo Hajdu,[△] Daniel Romo,[§] and Roberto G. S. Berlinck*[,†]

[†]Instituto de Química de São Carlos, Universidade de São Paulo, CP 780, CEP 13560-970, São Carlos, SP, Brazil

[§]Department of Chemistry & Biochemistry, Baylor University, Waco, Texas 76706, United States

[⊥]Instituto de Física de São Carlos, Avenida Joao Dagnone, 1100, Jardim Santa Angelina, São Carlos, SP, 13563-120, Brazil

[∥]Departamento de Biologia Animal e Departamento de Bioquímica e Biologia Tecidual, Instituto de Biologia, Universidade Estadual de Campinas, CEP 13083-862, Campinas, SP, Brazil

[▽]Departamento de Química, Universidade Federal de São Carlos, Rod. Washington Luiz, km 235 - SP-310, CEP 13565-905, São Carlos, SP, Brazil

[△]Museu Nacional, Universidade Federal do Rio de Janeiro, Quinta da Boa Vista, s/n, CEP 20940-040, Rio de Janeiro, RJ, Brazil

Supporting Information

ABSTRACT: The isolation and identification of a series of new pseudoceratidine (**1**) derivatives from the sponge *Tedania brasiliensis* enabled the evaluation of their antiparasitic activity against *Plasmodium falciparum*, *Leishmania* (*Leishmania*) *amazonensis*, *Leishmania* (*Leishmania*) *infantum*, and *Trypanosoma cruzi*, the causative agents of malaria, cutaneous leishmaniasis, visceral leishmaniasis, and Chagas disease, respectively. The new 3-debromopseudoceratidine (**4**), 20-debromopseudoceratidine (**5**), 4-bromopseudoceratidine (**6**), 19-bromopseudoceratidine (**7**), and 4,19-dibromopseudoceratidine (**8**) are reported. New tedamides A−D (**9**−**12**), with an unprecedented 4-bromo-4-methoxy-5-oxo-4,5-dihydro-1*H*-pyrrole-2-carboxamide moiety, are also described. Compounds **4** and **5**, **6** and **7**, **9** and **10**, and **11** and **12** have been isolated as pairs of inseparable structural isomers differing in their sites of bromination or oxidation. Tedamides **9**+**10** and **11**+**12** were obtained as optically active pairs, indicating an enzymatic formation rather than an artifactual origin. N^{12}-Acetylpseudoceratidine (**2**) and N^{12}-formylpseudoceratidine (**3**) were obtained by derivatization of pseudoceratidine (**1**). The antiparasitic activity of pseudoceratidine (**1**) led us to synthesize 23 derivatives (**16**, **17**, **20**, **21**, **23**, **25**, **27**−**29**, **31**, **33**, **35**, **38**, **39**, **42**, **43**, **46**, **47**, **50**, and **51**) with variations in the polyamine chain and aromatic moiety in sufficient amounts for biological evaluation in antiparasitic assays. The measured antimalarial activity of pseudoceratidine (**1**) and derivatives **4**, **5**, **16**, **23**, **25**, **31**, and **50** provided an initial SAR evaluation of these compounds as potential leads for antiparasitics against *Leishmania* amastigotes and against *P. falciparum*. The results obtained indicate that pseudoceratidine represents a promising scaffold for the development of new antimalarial drugs.

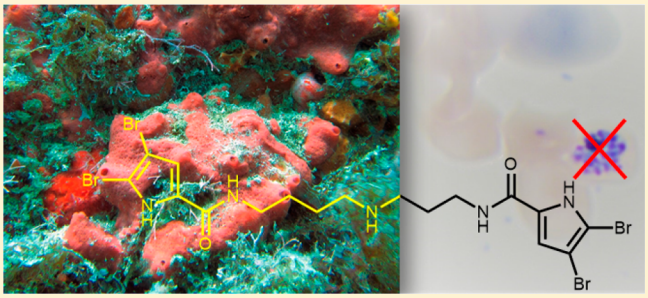

Bromopyrrole alkaloids isolated from marine sponges encompass a remarkable chemical diversity of potently bioactive compounds. These metabolites range from oroidin-related archetypal motifs to structurally complex oroidin-tetramers, the stylissadines.[1−3] Such alkaloids are prevalent in sponges belonging to the order Agelasida (particularly within the genus *Agelas*, family Agelasidae).[1−3] Nevertheless, several of these alkaloids have also been found in sponges of the genera *Axinella* (Axinellidae, Halichondrida), *Axinyssa* (Halichondriidae, Halichondrida), *Callyspongia* (Callyspongiidae, Haplosclerida), *Eurypon* (Raspailiidae, Poecilosclerida), *Hymeniacidon* (Halichondriidae, Halichondrida), and *Stylissa* (Halichondriidae, Halichondrida).[1−7] Therefore, past assumptions on the character of bromopyrrole alkaloids as chemotaxonomical markers of these sponges[4−7] are now challenged by their more widespread occurrence. Such is also the case for our present

Received: October 20, 2017

DOI: 10.1021/acs.jnatprod.7b00876
J. Nat. Prod. XXXX, XXX, XXX−XXX

Chart 1

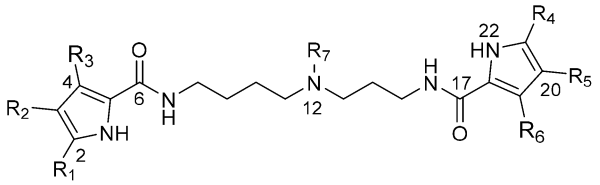

1 $R_1 = R_2 = R_4 = R_5 = Br$, $R_3 = R_6 = R_7 = H$
2 $R_1 = R_2 = R_4 = R_5 = Br$, $R_3 = R_6 = R_7 = C(O)CH_3$
3 $R_1 = R_2 = R_4 = R_5 = Br$, $R_3 = R_6 = R_7 = C(O)H$
4 $R_1 = R_4 = R_5 = Br$, $R_2 = R_3 = R_6 = R_7 = H$
5 $R_1 = R_2 = R_4 = Br$, $R_3 = R_5 = R_6 = R_7 = H$
6 $R_1 = R_2 = R_3 = R_4 = R_5 = Br$, $R_6 = R_7 = H$
7 $R_1 = R_2 = R_4 = R_5 = R_6 = Br$, $R_3 = R_7 = H$
8 $R_1 = R_2 = R_3 = R_4 = R_5 = R_6 = Br$, $R_7 = H$

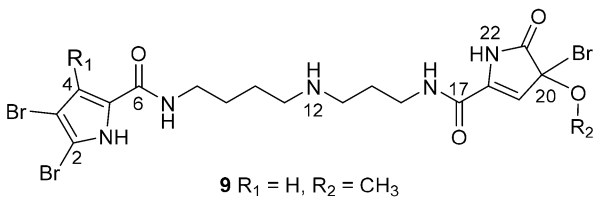

9 $R_1 = H$, $R_2 = CH_3$
11 $R_1 = Br$, $R_2 = CH_3$

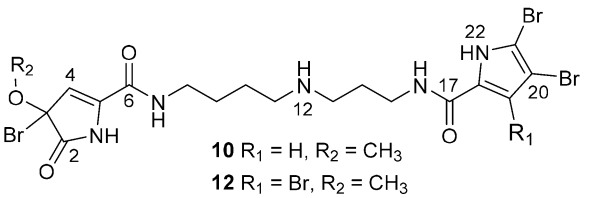

10 $R_1 = H$, $R_2 = CH_3$
12 $R_1 = Br$, $R_2 = CH_3$

Table 1. ^{1}H NMR Data (δ, ppm) for Pseudoceratidines 2−8 in DMSO-d_6

position	**2**[b] (J in Hz)	**3**[b] (J in Hz)	**4**[a] (J in Hz)	**5**[a] (J in Hz)	**6**[b] (J in Hz)	**7**[b] (J in Hz)	**8**[b] (J in Hz)
N−H	12.60, br s	12.63/12.61, s	12.18, br s	12.63, d (2.2)	n.o.	n.o.	n.o.
2							
3			6.72, dd (2.5, 2.7)				
4	6.86, m	6.88/6.87, s	6.11, dd (2.5, 3.7)	6.89, d (2.2)		6.89, s	
5							
6							
N−H	8.06, t (5.6)/8.04, m	8.10, m	8.03, t (5.7)	8.14, t (5.7)	7.76, t (6.1)	8.14, t (5.6)	7.34, br t
8	3.19, m	3.21/3.17, m	3.20, m	3.20, m	3.25, m	3.21, m	3.16, m
9	1.47/1.41, m	1.40/1.37, m	1.52, m	1.52, m	1.53, m	1.52, m	1.48, m
10	1.53/1.45, m	1.49/1.45, m	1.57, m	1.57, m	1.58, m	1.58, m	1.57, m
11	3.24/3.21, m	3.24/3.20, m	2.90, br m	2.90, br m	2.90, m	2.89, m	2.88, t (7.4)
N−H	n.o.	n.o.	n.o.	n.o.	n.o.	n.o.	n.o.
13	3.25/3.24, m	3.23/3.22, m	2.90, br m	2.90, br m	2.90, m	2.86, m	2.83, t (7.4)
14	1.73/1.64, m	1.68/1.64, m	1.77, m	1.77, m	1.79, m	1.76, m	1.73, m
15	3.17, m	3.16/3.15, m	3.25, m	3.25, m	3.29, m	3.25, m	3.20, q (6.2)
N−H	8.09, t (5.6)/8.04, m	8.10, m	8.24, t (6.0)	8.15, t (5.7)	8.24, t (5.6)	7.72, t (6.0)	7.61, t (6.0)
17							
18							
19	6.89, m	6.88/6.87, s	6.90, d (2.2)	6.13, dd (2.5, 3.7)	6.90 s		
20				6.71, dd (2.5, 2.7)			
21							
N−H	12.60, br s	12.63/12.61, s	12.67, d (2.2)	12.13, br s	n.o.	n.o.	n.o.
23		8.00/7.99, s					
24	1.97/1.94, s						

[a]400 MHz. [b]600 MHz; n.o.: not observed; ^{1}H signals for the HCO_2^- counterion observed between δ_H 8.12 and 8.33 for all compounds.

isolation of pseudoceratidine (**1**) derivatives from the marine sponge *Tedania brasiliensis* (Tedaniidae, Poecilosclerida).

Pseudoceratidine (**1**) was previously isolated solely from the sponge *Pseudoceratina purpurea* (Pseudoceratinidae, Verongida).[8,9] The compound displayed more potent antifouling activity than its monosubstituted 4,5-dibromo-1*H*-pyrrole-2-carboxylic acid spermidine analogues.[10] In these previous studies, it was found that both the substitution pattern of the terminal rings and the length of the triamine chain of pseudoceratidine derivatives affect the antifouling activity. Furthermore, pseudoceratidine also displayed the most potent antibacterial activity against *Staphylococcus aureus*, *Listeria monocytogenes*, *Pseudomonas aeruginosa*, *Escherichia coli*, and *Serratia liquefaciens*.[11] In the present investigation, we report the antiparasitic activity of pseudoceratidine and several new synthetic pseudoceratidine derivatives against *Plasmodium falciparum*, *Leishmania (Leishmania) amazonensis*, *L.* (*L.*) *infantum*, and *Trypanosoma cruzi*.

Malaria, caused by *Plasmodium* spp., is among the most devastating vector-born human infectious diseases. It is estimated that over 3.4 billion people worldwide are at risk of infection. Malaria is prevalent in tropical and subtropical regions, affecting 212 million people and causing 429 000 deaths in 2015. In Africa, *P. falciparum* is responsible for the highest mortality rate of children under 5 years of age. Malaria etiologic agents have developed resistance to several antimalarial drugs, including emerging resistance to artemisinin and artemisinin-based combination therapies that comprise current first-line treatments.[12] Thus, the discovery of new antimalarial lead compounds is of utmost importance.

Leishmaniasis is a group of diseases caused by several species of protozoan parasites belonging to the genus *Leishmania*

DOI: 10.1021/acs.jnatprod.7b00876
J. Nat. Prod. XXXX, XXX, XXX−XXX

Table 2. ^{13}C NMR Data (δ, ppm) for Pseudoceratidines 2−8 in DMSO-d_6

position	2[b] δ_C, type	3[b] δ_C, type	4[a] δ_C, type	5[a] δ_C, type	6[b] δ_C, type	7[b] δ_C, type	8[b] δ_C, type
2	104.6, C	104.77/104.68, C	102.7, C	104.7, C	n.o.	104.6, C	n.o.
3	97.9, C	98.09/98.07, C	111.7, CH	98.0, C	n.o.	97.9, C	n.o.
4	112.5, CH	112.8/112.6, CH	111.0, CH	112.9, CH	n.o.	112.6, CH	n.o.
5	128.4, C	128.53/128.47, C	128.4, C	128.0, C	n.o.	128.3, C	n.o.
6	158.93/159.0, C	159.2/159.15, C	159.9, C	159.4, C	n.o.	159.1, C	162.8, C
8	38.5/38.3, CH_2	38.5/38.3, CH_2	38.0, CH_2	37.9, CH_2	38.3, CH_2	38.0, CH_2	37.3, CH_2
9	26.8/26.6, CH_2	26.8/26.4, CH_2	26.52, CH_2	26.6, CH_2	26.37, CH_2	26.5, CH_2	27.0, CH_2
10	26.0/25.0, CH_2	25.8/24.5, CH_2	23.3, CH_2	23.4, CH_2	23.31, CH_2	23.3, CH_2	23.4, CH_2
11	47.8/44.5, CH_2	46.4/40.1, CH_2	46.8, CH_2	46.9, CH_2	46.80, CH_2	46.7, CH_2	46.9, CH_2
13	45.8/42.7, CH_2	44.2/41.0, CH_2	45.07, CH_2	45.09, CH_2	44.9, CH_2	44.7, CH_2	44.8, CH_2
14	28.8/27.8, CH_2	28.2/27.4, CH_2	26.4, CH_2	26.57, CH_2	26.2, CH_2	26.5, CH_2	26.9, CH_2
15	36.5/36.3, CH_2	36.6/36.0, CH_2	36.0, CH_2	35.8, CH_2	36.0, CH_2	35.3, CH_2	34.8, CH_2
17	158.95/159.1, C	159.2/159.13, C	159.1, C	160.2, C	159.4, C	162.0, C	163.9, C
18	128.3, C	128.50/128.41, C	128.1, C	128.3, C	128.3, C	n.o.	n.o.
19	112.4, CH	112.8/112.6, CH	112.7, CH	111.1, CH	112.8, CH	n.o.	n.o.
20	97.9, C	98.09/98.07, C	98.1, C	112.0, CH	98.0, C	n.o.	n.o.
21	104.5, C	104.75/104.63, C	104.9, C	102.4, C	104.6, C	n.o.	n.o.
23	169.6/169.3, C	163.2/163.1, CH					
24	21.4/21.3, CH_3						

[a]100 MHz. [b]150 MHz; n.o.: not observed.

endemic in more than 80 countries.[13] Transmitted by different sandfly species, *Leishmania* parasites infect cells from the mononuclear phagocytic system, leading to clinical manifestations that vary from localized, disseminated, and diffuse skin lesions (cutaneous leishmaniasis) to a systemic multiorgan infection (visceral leishmaniasis). Visceral leishmaniasis is fatal if left untreated. Treatment options are limited to parenteral drugs, including pentavalent antimonials as the first-line drugs, which very often present severe side effects. The utilization of liposomal amphotericin B and oral miltefosine proved useful for treating patients with visceral leishmaniasis. Nevertheless, the high cost of liposomal amphotericin B and the miltefosine teratogenic effect, in addition to its long half-life, hampers the therapeutic success of such treatments.[14,15] Therefore, the identification of new drug candidates for leishmaniasis treatment remains imperative in the current therapeutic scenario.

T. cruzi is the causative agent of Chagas disease, which may lead to fatal disorders such as cardiomegaly and megacolon in approximately 30% of patients.[16] The disease is an emerging health issue in North America and Europe.[17−19] Approximately 8−10 million people in Latin American countries are infected by *T. cruzi*, with an annual death rate of approximately 14 000 people.[18,19] Benznidazole, toxic and of limited efficacy, is the only available therapy in Brazil for Chagas disease. No effective treatment exists for chronic phase patients affected by Chagas disease.[20] Thus, the discovery of new therapies for Chagas disease is sorely needed. Furthermore, there are no approved vaccines for the treatment of humans to prevent malaria, leishmaniasis, or Chagas disease.

In our continuing search for antiparasitic marine metabolites,[21−24] we verified that the MeOH antiparasitic extract of *T. brasiliensis* contained pseudoceratidine (**1**) as the most abundant metabolite. Related minor constituents were detected only by HPLC-UV-MS because of the high abundance of **1** in the sponge extract. Several chromatographic separations of this extract yielded a series of minor pseudoceratidine derivatives. These include the new tedamides A−D (**9**−**12**), along with the new 3-debromopseudoceratidine (**4**), 20-debromopseudoceratidine (**5**), 4-bromopseudoceratidine (**6**), 19-bromopseudoceratidine (**7**), and 4,19-dibromopseudoceratidine (**8**). Compounds **4** and **5**, **6** and **7**, **9** and **10**, as well as **11** and **12** have been isolated as pairs of inseparable structural isomers differing in their sites of bromination or oxidation. Since pseudoceratidine displayed good anti-*P. falciparum* activity, we prepared a series of pseudoceratidine derivatives with different polyamine and aromatic moieties, aiming to assess their anti-*P. falciparum*, anti-*Leishmania* spp., and anti-*T. cruzi* activities and begin evaluation of their structure−activity relationships.

RESULTS AND DISCUSSION

Isolation and Identification of Natural Pseudoceratidine Derivatives. Analysis of the HRMS and NMR data of **1**[8,9] facilitated the identification of minor pseudoceratidine congeners **4**−**12** (Tables 1−4) that were all isolated as their formate salts. The inseparable mixture of 3-debromopseudoceratidine (**4**) and 20-debromopseudoceratidine (**5**) displayed a protonated molecule cluster at *m/z* 565.9409/567.9389/569.9370/571.9354 with peaks showing relative intensities of 1:3:3:1. The $[M + H]^+$ ion at *m/z* 565.9409 corresponded to the formula $C_{17}H_{23}{}^{79}Br_3N_5O_2$, with one fewer bromine atom and one more hydrogen atom than **1**. Monobromo substitution at one of the pyrrole moieties was verified in the COSY spectrum of **4** and **5**. Coupling between two hydrogens was observed in one of the pyrrole rings, at δ_H 6.11/6.13 (dd, J = 2.5 and 3.7 Hz, H-4 or H-19) and at δ_H 6.71/6.72 (dd, J = 2.5 and 2.7 Hz, H-3 or H-20), both of which coupled with an NH group at δ_H 12.13/12.18 (br s). A doublet at δ_H 6.89/6.90 (d, J = 2.2 Hz, H-4 or H-19) was assigned to the hydrogen of a 2,3-dibromo-substituted pyrrole group, which coupled only to the NH group at δ_H 12.67/12.63 (d, J = 2.2 Hz). Analysis of the COSY spectrum of **4** indicated that H-4 (δ_H 6.11, dd, J = 2.5 and 3.7 Hz) was vicinal to H-3 (δ_H 6.72, dd, J = 2.5 and 2.7 Hz). In the HMBC spectrum, H-4 coupled with C-2 (δ_C 102.7), C-5 (δ_C 128.4), and C-6 (δ_C 159.9), whereas NH-7 (δ_H 8.03, t, J = 5.7 Hz) coupled with C-6 and C-8 (δ_C 38.0). These couplings indicated that in **4** the monobromopyrrole-2-

DOI: 10.1021/acs.jnatprod.7b00876
J. Nat. Prod. XXXX, XXX, XXX−XXX

Table 3. ^{1}H NMR Data (δ, ppm) for Tedamides A–D (9–12) in DMSO-d_6

position	9[a] (J in Hz)	10[a] (J in Hz)	11[b] (J in Hz)	12[b] (J in Hz)
N–H	12.63, d (1.6)	9.07, d (1.6)	n.o.	9.07, br
2				
3				
4	6.90, m	7.30, d (1.6)		7.29, s
5				
6				
N–H	8.14, t (5.7)	8.28, m	7.54, t (5.8)	8.27, t (5.9)
8	3.21, m	3.08, m	3.21, m	3.10, m
9	1.49, m	1.46, m	1.54, m	1.48, m
10	1.53, m	1.57, m	1.58, m	1.54, m
11	2.88, br	2.88, m	2.88, m	2.88, m
N–H	n.o.	n.o.	n.o.	n.o.
13	2.88, br	2.88, m	2.85, m	2.85, m
14	1.73, m	1.78, m	1.74, m	1.77, m
15	3.11, m	3.26, m	3.15, m	3.26, m
N–H	8.39, t (6.0)	8.25, m	8.39, t (5.9)	7.71, t (6.0)
17				
18				
19	7.34, d (1.7)	6.90, m	7.33, s	
20				
21				
N–H	9.09, d (1.5)	12.67, d (1.4)	9.08, br	n.o.
O–CH_3	3.18, s	3.17, s	3.17, s	3.16, s

[a]400 MHz. [b]600 MHz; n.o.: not observed.

Table 4. ^{13}C NMR Data (δ, ppm) for Tedamides A–D (9–12) in DMSO-d_6

position	9[a] δ_C, type	10[a] δ_C, type	11[b] δ_C, type	12[b] δ_C, type
2	104.6, C	167.1, C	n.o.	167.3, C
3	97.9, C	92.1, C	n.o.	92.29, C
4	112.6, CH	144.5, CH	n.o.	144.73, CH
5	128.3, C	121.5, C	n.o.	121.71, C
6	159.0, C	165.6, C	160.4, C	165.8, C
8	38.0, CH_2	38.7, CH_2	37.9, CH_2	38.8, CH_2
9	26.4, CH_2	26.1, CH_2	26.67, CH_2	26.1, CH_2
10	23.2, CH_2	23.1, CH_2	23.3, CH_2	23.2, CH_2
11	46.7, CH_2	46.6, CH_2	46.9, CH_2	46.7, CH_2
13	44.7, CH_2	44.9, CH_2	44.9, CH_2	44.8, CH_2
14	25.8, CH_2	26.3, CH_2	25.9, CH_2	26.6, CH_2
15	36.5, CH_2	35.9, CH_2	36.6, CH_2	35.5, CH_2
17	166.0, C	159.3, C	166.2, C	162.0, C
18	121.6, C	128.1, C	121.79, C	n.o.
19	144.5, CH	112.8, CH	144.72, CH	n.o.
20	92.0, C	98.0, C	92.21, C	n.o.
21	167.2, C	104.8, C	167.4, C	n.o.
23	51.1, CH_3	51.1, CH_3	51.3, CH_3	51.3, CH_3

[a]100 MHz. [b]150 MHz; n.o.: not observed.

carboxylic acid group was attached to the NH amide connected to the four-methylene moiety of spermidine, because H_2-8 showed couplings to H_2-9 in the COSY spectrum and to C-9 and C-10 in the HMBC spectrum. Considering the NMR data of **4**, the dibromopyrrole-2-carboxylic acid group had to be attached to the three-methylene moiety of spermidine. Indeed, H-19 (δ_H 6.90, d, J = 2.2 Hz) coupled with C-18 (δ_C 128.1) and with C-21 (δ_C 104.9), whereas NH-16 (δ_H 8.24, t, J = 6.0 Hz) coupled with C-15 (δ_C 36.0) and C-17 (δ_C 159.1). In the HMBC spectrum, the isomeric compound **5** shows H-4 (δ_H 6.89, d, J = 2.2 Hz) at the dibromopyrrolecarboxylic acid group coupling with C-2 (δ_C 104.7), C-5 (δ_C 128.0), and C-6 (δ_C 159.4), whereas NH-7 (δ_H 8.14, t, J = 5.7 Hz) coupled with C-6 at δ_C 159.4 and with C-8 (δ_C 37.9). At the other end of the spermidine chain of **5**, H-19 (δ_H 6.13, dd, J = 2.2 and 3.7 Hz) showed a coupling with H-20 (δ_H 6.71, dd, J = 2.5 and 2.7 Hz) in the COSY spectrum and coupled with C-18 (δ_C 128.3) and with C-21 (δ_C 102.4) in the HMBC spectrum. Unambiguous ^{1}H and ^{13}C assignments were also based on the relative integration of the ^{1}H signals of **4** and **5**, those of **4** being slightly higher than those of **5**, with a relative abundance of approximately 55/45, respectively. The ^{1}H and ^{13}C signals for the methylene groups of the spermidine chain were essentially the same for **4** and **5** (Tables 1 and 2) and identical to those of **1**. Thus, the structures of 3-debromopseudoceratidine (**4**) and 20-debromopseudoceratidine (**5**) were established.

A fraction presenting an inseparable mixture of the isomeric 4-bromopseudoceratidine (**6**) and 19-bromopseudoceratidine (**7**) was obtained along with one distinct fraction providing pure **7**. Many attempts made to separate both **6** and **7** under different HPLC conditions were unsuccessful. The HRMS spectrum of the mixture of **6** and **7**, as well as that of pure **7**, displayed a protonated molecule cluster at m/z 721.7632/723.7587/725.7626/727.7581/729.7564/731.7520, with peaks showing relative intensities of 1:5:10:10:5:1. The $[M + H]^+$ ion at m/z 721.7632 corresponded to the formula $C_{17}H_{21}{}^{79}Br_5N_5O_2$, with one more bromine atom and one fewer hydrogen atom than **1**. The ^{1}H NMR spectrum of **7** (Table 1) presented a singlet at δ_H 6.89 integrating to one ^{1}H (H-4), indicating that one of the pyrrole moieties was substituted by three bromines. The HMBC spectrum of **7** showed couplings of H-4 with C-2 (δ_C 104.6), C-3 (δ_C 97.9, weak), C-5 (δ_C 128.3), and C-6 (δ_C 159.1), as well as between NH-7 (δ_H 8.14, br t, J = 5.6 Hz) and C-6 and C-8 (δ_C 38.0), which enabled us to establish to which of the two amides the dibrominated pyrrole moiety was attached. Because the H_2-8 methylene protons (δ_H 3.21) showed HMBC couplings to C-9 (δ_C 26.5) and to C-10 (δ_C 23.3), whereas H_2-11 (δ_H 2.89) showed couplings to C-10, C-9, and C-13 (δ_C 44.7), it was possible to determine the connectivity of the 2,3-dibromopyrrole-5-carboxylic acid group to NH-7 in compound **7**. Additional HMBC couplings between NH-16 (δ_H 7.72) and C-17 (δ_C 162.0) and C-15 (δ_C 35.3) and between H_2-15 (δ_H 3.25) and C-14 (δ_C 26.5) and C-13, along with couplings observed between H_2-13 (δ_H 2.86) and C-11, C-14, and C-15, confirmed the structure of 19-bromopseudoceratidine (**7**). Finally, MS/MS analysis of **7** provided further support for its structure (Figures S30 and S31, Supporting Information). Fragment ions detected at m/z 395.0079, 397.0097, 399.0098 (1:2:1) and at m/z 320.9235, 322.9219, 324.9187 (1:2:1) indicated that the dibromopyrrole-2-carboxylic acid group was attached to the four-methylene amine moiety of **7**, whereas fragment ions observed at m/z 498.9012, 500.8963, 502.8913 (1:3:3:1), at m/z 472.9718, 474.9163, 476.9141, 478.9121 (1:3:3:1), and at m/z 384.8184, 386.8165, 388.8146, 390.8121 (1:3:3:1) indicated that the tribromopyrrole-2-carboxylic acid group was attached to the three-methylene amine moiety of **7**, confirming its structure with no ambiguity.

The assignments of ^{1}H and ^{13}C NMR signals of **6** were also established by analysis of NMR data obtained for the 50/50 mixture of **6** and **7** (Tables 1 and 2). For compound **6**, the singlet at δ_H 6.90 (H-19) showed couplings in the HMBC

DOI: 10.1021/acs.jnatprod.7b00876
J. Nat. Prod. XXXX, XXX, XXX–XXX

spectrum with C-17 (δ_C 159.4), C-18 (δ_C 128.3), and C-21 (δ_C 104.6). The amide NH-16 (δ_H 8.24, t, J = 5.6 Hz) showed couplings with C-17 and C-15 (δ_C 36.0), whereas CH_2-15 (δ_H 3.29) showed couplings with C-17 (δ_C 159.4), C-14 (δ_C 26.2), and C-13 (δ_C 44.9) in the HMBC spectrum. In the COSY spectrum, H_2-15 was coupled with NH-16 and H_2-14 (δ_H 1.79), which was sequentially coupled with H_2-13 (δ_H 2.90). The remaining four-methylene chain was shown to be attached to the NH-7/C-6 amide group. Complete assignments of ^{1}H and ^{13}C resonances of **6** and **7** (Tables 1 and 2) enabled the identification of these pentabrominated alkaloids.

The structure of 4,19-dibromopseudoceratidine (**8**) could be established by HRMS analysis, which showed a protonated molecule cluster at m/z 799.6352/801.6241/ 803.6213/ 805.6219/ 807.6194/809.6263/ 811.6205 with peaks showing relative intensities of 1:6:15:20:15:6:1. The $[M + H]^+$ ion at m/z 799.6352 corresponded to the formula $C_{17}H_{20}{}^{79}Br_6N_5O_2$, with two more bromine atoms and two fewer hydrogen atoms than **1**. Inspection of ^{1}H NMR data obtained for **8** revealed that it corresponded to the 4,19-dibrominated version of **1**, because no pyrrole hydrogen was detected, whereas the ^{1}H signals of the spermidine chain remained very similar to the corresponding ^{1}H signals in compounds **1**−**7**. The same pattern was observed for the ^{13}C NMR signals of **8** (Tables 1 and 2). Therefore, the structure of **8** was established as that of 4,19-dibromopseudoceratidine.

Isomeric tedamides A (**9**) and B (**10**) were isolated as an inseparable mixture and presented a protonated molecule cluster at m/z 611.9452/613.9453/ 615.9435/617.9399, with peaks showing relative intensities of 1:3:3:1. The $[M + H]^+$ ion at m/z 611.9452 corresponded to the formula $C_{18}H_{25}{}^{79}Br_3N_5O_4$, with eight double-bond equivalents. A set of doubled signals in the ^{13}C NMR spectrum (Table 4) indicated the presence of two closely related compounds. Several attempts to separate them by HPLC using different columns and/or solvent mixtures failed. Because the intensities of the ^{13}C NMR signal pairs were not identical, we assumed a mixture of a slightly major isomer (**10**) and a minor one (**9**), in 55:45 relative ratio. The assignments of the tedamide B isomer (**10**) were established as follows.

The β,γ-unsaturated lactam moiety in **10** was constructed by analysis of the HMBC spectrum. Correlations between NH-1 (δ_H 9.07) and C-2 (δ_C 167.1), C-3 (δ_C 92.1), C-4 (δ_C 144.5), and C-5 (δ_C 121.5), between H-4 (δ_H 7.30, d, J = 1.6 Hz) and C-2, C-3, and C-5, and between the methoxy group at δ_H 3.17 and C-3 accounted for either one of the two hypothetical lactam moieties, A or B (Figure 1). Fragment B was discarded because the coupling constant observed for H-4 (J = 1.6 Hz) agrees with a long-distance ^{1}H−^{1}H coupling rather than a vicinal ^{1}H−^{1}H coupling between H-4 and NH-1. Moreover, analysis of the 1D NOESY spectrum of the mixture of **9** and **10** showed a strong NOE between H-4 and the methoxy group. The ^{13}C signals of sp^2 carbons of **9** and **10** were assigned to a 2,3-dibromopyrrole moiety by comparison with data for **1**.[8] ^{1}H and ^{13}C NMR assignments of the spermidine chain were based on the higher intensity of the ^{13}C NMR signals of **10**, by analysis of COSY and HMBC spectra as well as by comparison with data for **1**. Because ^{13}C chemical shifts of the pyrrole conjugated amide carbons lie below δ_C 160, for tedamide B (**10**) C-6 was assigned at δ_C 165.6 and C-17 at δ_C 159.3. Couplings of NH-16 (δ_H 8.25) with C-17 and C-15 (δ_C 35.9) and of NH-7 (δ_H 8.28) with C-6 and C-8 (δ_C 38.7) confirmed such assignments (Tables 3 and 4). Analogous reasoning enabled the identification of tedamide A (**9**) as the minor isomer of **10**.

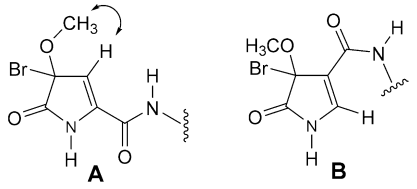

Figure 1. NOE observed in the 1D NOESY spectrum of tedamides A (**9**) and B (**10**) that supports the presence of fragment A instead of fragment B in the structures of **9** and **10**.

Tedamides C (**11**) and D (**12**) were also isolated as inseparable isomers in a ratio of approximately 28:72, presenting a protonated molecule cluster at m/z 689.8571/ 691.8551/ 693.8535/695.8514/ 697.8499 with peaks showing relative intensities of 1:4:6:4:1. The $[M + H]^+$ ion at m/z 689.8571 corresponded to the formula $C_{18}H_{24}{}^{79}Br_4N_5O_4$, with one more bromine atom than tedamides A and B. Analysis of the NMR data of **11** and **12** indicated that the hydrogen at the pyrrole moiety was missing, whereas the remaining structures were essentially identical to those of compounds **9** and **10** (Tables 3 and 4). Thus, the structures of tedamides **11** and **12** were assigned as those corresponding to the tribrominated pyrrole derivatives of **9** and **10**.

α-Bromo-α-alkoxyamides are known stable chemical entities, frequently utilized as functionalized substrates suitable for the preparation of further derivatives in medicinal chemistry.[25−30] However, we have been unable to find β,γ-unsaturated-α-bromo-α-alkoxy lactams in the literature or any natural product bearing such functionalities in the SciFinder, Dictionary of Natural Products, or MarinLit natural products databases. Thus, the 4-bromo-4-methoxy-5-oxo-4,5-dihydro-1*H*-pyrrole-2-carboxamide moieties of tedamides A and B are structurally unprecedented. Although an artifactual origin could, in principle, be considered for tedamides given that MeOH was used as the extraction solvent, the mixture of compounds **9** and **10** displayed some optical activity ($[\alpha]_D$ −7.8 (c 0.007, MeOH)), while the mixture of **11** and **12** displayed significant optical activity ($[\alpha]_D$ +110 (c 0.0006, MeOH)). This provides evidence that these bromomethoxy acetals are not artifacts of oxidation during the isolation process but are likely products of an enzymatic oxidation.

The isolation of tri-, tetra-, penta-, and hexabrominated pyrrole alkaloids from *T. brasiliensis* is noteworthy. Prior to the present investigation, the 3,4,5-tribromo-1*H*-pyrrole-2-carboxylic acid was the only alkaloid presenting a tribromo acylpyrrole isolated from a marine sponge, *Axinella* sp.[31] Because several bromine-substituted pyrroles have been isolated from cultures of marine bacteria,[32,33] it is possible that sponge polybrominated pyrrole alkaloids may have a bacterial origin. However, recent investigations have shown that vanadium-dependent bromoperoxidases isolated from marine algae promote bromination of a variety of pyrrole derivatives,[34−36] including that of 1*H*-pyrrole-2-carboxamide and 1*H*-pyrrole-2-carboxylate esters, which are commonly found in Agelasida and other marine sponges. Therefore, the distribution of brominated pyrroles in nature may be related not only to the diversity of bacteria associated with macroorganisms but possibly also to a widespread occurrence of bromoperoxidases in phylogenetically distant taxa. A recent

DOI: 10.1021/acs.jnatprod.7b00876
J. Nat. Prod. XXXX, XXX, XXX−XXX

Scheme 1. Syntheses of Pseudoceratidine Derivatives with Variations in the Tether

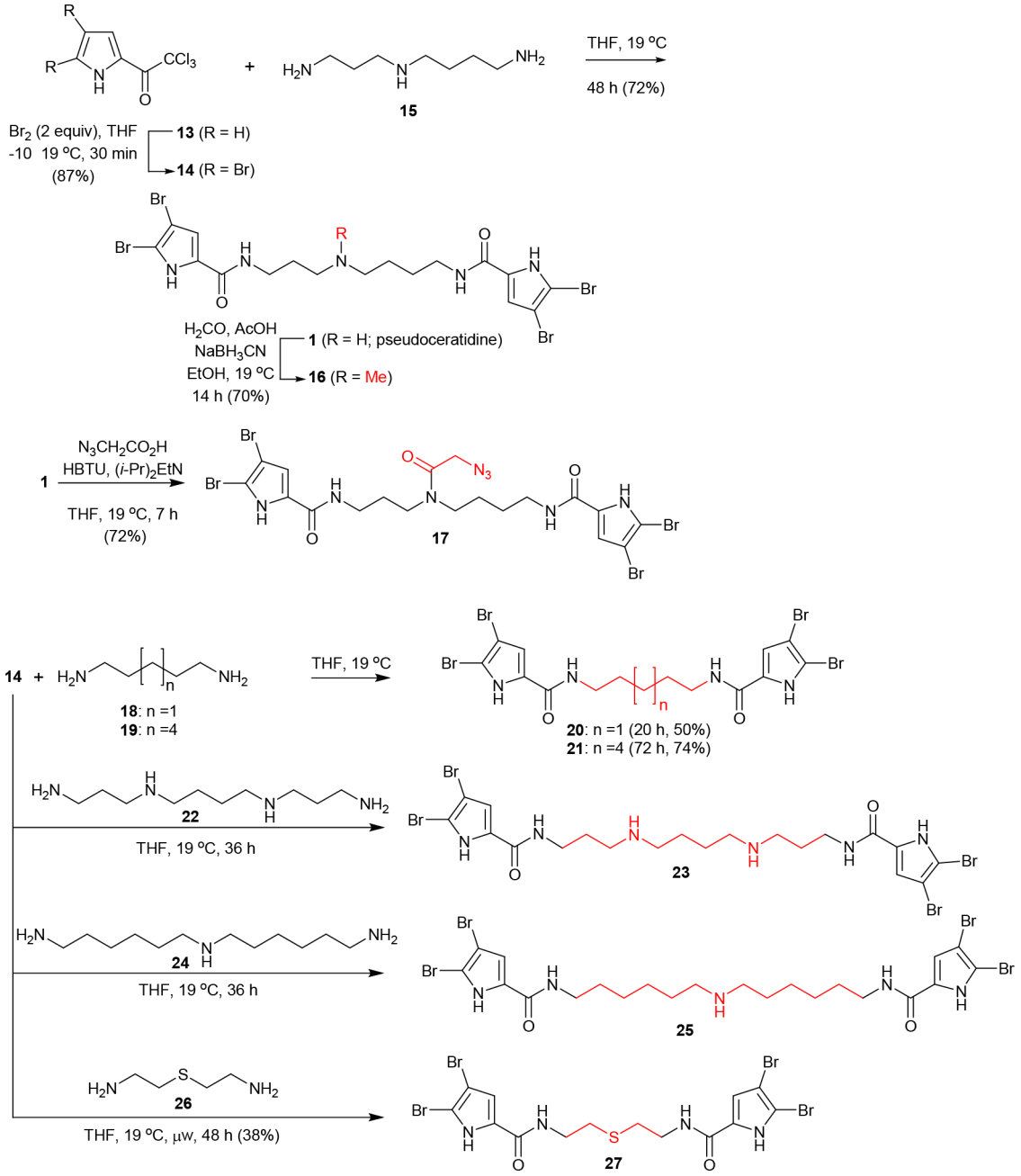

metagenomic analysis of *T. brasiliensis* and other sponges presenting bromopyrrole alkaloids indicates that the biosynthesis of these compounds is related to the less abundant microbes in these sponges.[37]

Derivatization of Pseudoceratidine and Synthesis of Pseudoceratidine Derivatives. Aiming to evaluate structure−activity relationships of pseudoceratidine and congeners in antiparasitic assays, a series of 23 pseudoceratidine derivatives were synthesized. Natural pseudoceratidine was acetylated with Ac_2O in pyridine to obtain its N^{12}-acetyl derivative (**2**). After HPLC purification of the acetylated product, we obtained both N^{12}-acetylpseudoceratidine (**2**) and N^{12}-formylpseudoceratidine (**3**). Compound **3** is likely derived from reaction of pseudoceratidine with acetic formic anhydride resulting from the reaction of Ac_2O and residual formic acid from the HPLC solvent used to purify pseudoceratidine. Compounds **2** and **3** were fully characterized by HRMS, ^{1}H, ^{13}C, HSQC, and HMBC spectra (Supporting Information).

In order to prepare additional pseudoceratidine derivatives in sufficient amounts for testing in several antiparasitic assays, the natural product was first synthesized based on a previously reported procedure.[10,11] Commercially available 2,2,2-trichloro-1-(1*H*-pyrrol-2-yl)ethenone (**13**) was brominated with Br_2 to give the known dibrominated pyrrole **14**[38] in 87% yield. Coupling of **14** with spermidine (**15**) in tetrahydrofuran provided synthetic pseudoceratidine in 72% yield (Scheme 1). *N*-Methylpseudoceratidine (**16**) was then prepared by reductive amination with formaldehyde in 70% yield to probe the importance of the basic secondary amine as a proton donor or acceptor, or both. Toward a derivative (**17**) amenable to further coupling with a fluorophore via

DOI: 10.1021/acs.jnatprod.7b00876
J. Nat. Prod. XXXX, XXX, XXX−XXX

Scheme 2. Syntheses of Pseudoceratidine Derivatives with Variations in the Pyrrole (Aromatic) Moiety

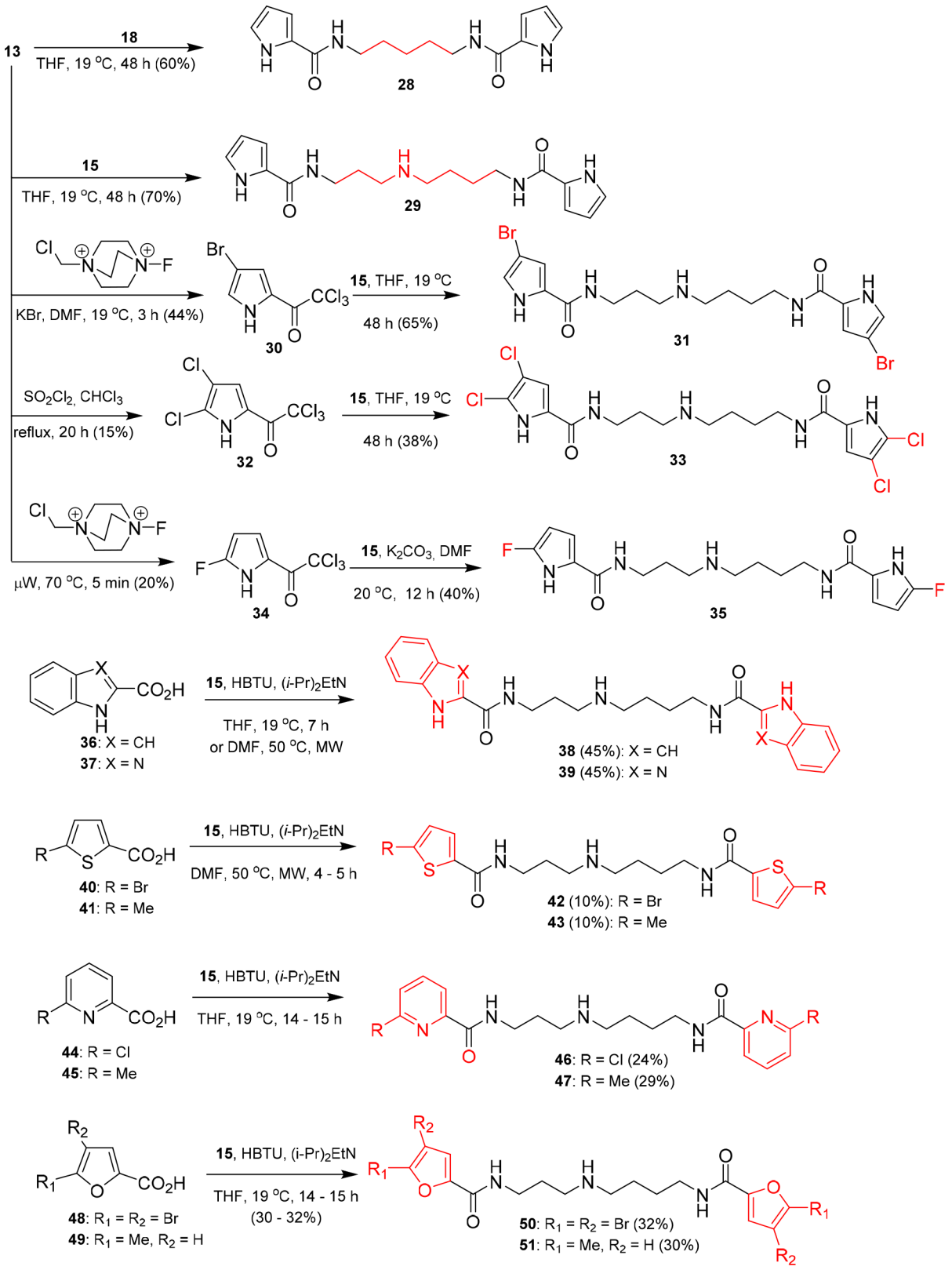

Sharpless–Hüisgen cycloaddition, pseudoceratidine (**1**) was coupled to 2-azidoacetic acid in 72% yield (Scheme 1).

A series of derivatives with different chains between the two pyrrole moieties were also synthesized to probe the importance of the chain length and the requirement of basic amines (Scheme 1). Compounds **20** and **21** were prepared using the same conditions for the preparation of **1** employing 1,5-diaminopentane or 1,8-diaminooctane, in 50% and 74% yield from **14**, respectively. Pseudoceratidine derivatives **23** and **25** were prepared using similar conditions with spermine (**22**) and

DOI: 10.1021/acs.jnatprod.7b00876
J. Nat. Prod. XXXX, XXX, XXX–XXX

Table 5. Antileishmanial, Anti-*Trypanosoma cruzi*, Anti-Plasmodial, and Cytotoxicity Activities of Pseudoceratidine Derivatives[a]

	L. infantum promastigotes	*L. amazonensis* promastigotes	*T. cruzi* epimastigotes	bone-marrow-derived macrophages	*P. falciparum* (3D7)	HepG2	
compd	EC_{50} ± SD (μM)	EC_{50} ± SD (μM)	EC_{50} ± SD (μM)	CC_{50} ± SD (μM)	EC_{50} ± SD (μM)	MDL_{50} ± SD (μM)	selectivity index[b]
1	>100	>100	>100	–	1 ± 0.1 (0.96–1.24)	16 ± 1 (14.6–17.4)	15
2	>100	>100	>100	–	>10	–	–
4 + 5	>100	>100	>100	–	6 ± 1 (5.11–6.49)	≥400	≥69
9 + 10	>100	>100	>100	–	>100	–	–
16	>100	>100	>100	–	4 ± 1 (3–6)	160 ± 23 (128–192)	35
17	>100	>100	>50	–	>10	–	–
20	24 ± 3 (20–27)	19 ± 1 (18–20)	7 ± 1 (5–7)	52 ± 3 (49–55)	>10	–	–
21	>100	>100	>100	–	>10	–	–
23	19 ± 1 (17–20)	44 ± 5 (38–49)	>100	>100	2 ± 1 (0.20–3)	99 ± 12 (82–116)	52
25	>100	>100	>100	–	3 ± 1 (2–3)	263 ± 43 (203–323)	101
27	24 ± 3 (21–28)	43 ± 2 (41–45)	24 ± 4 (21–27)	66 ± 5 (61–72)	>10	–	–
28	>100	>100	>50	–	>10	–	–
29	>100	>100	>100	–	>10	–	–
31	>100	>100	>100	–	7 ± 1 (6–8)	≥400	≥54
33	>100	>100	>100	–	>10	–	–
35	>100	>100	>100	–	>10	–	–
38	>100	>100	>100	–	>10	–	–
39	>100	>100	>100	–	>10	–	–
42	20 ± 3 (17–24)	76 ± 2 (72–80)	>100	>100	>10	–	–
43	>100	>100	>100	–	>10	–	–
46	>100	>100	>100	–	>10	–	–
47	>100	>100	>100	–	>10	–	–
50	23 ± 5 (17–28)	18 ± 2 (16–19)	>100	82 ± 4 (78–87)	3 ± 1 (2–4)	≥400	≥125
51	>100	>100	>100	–	>10	–	–

[a]EC_{50}: half-maximal effective concentration; CC_{50}: half-maximal cytotoxic concentration; S.D.: standard deviation; 95% confidence interval values are shown in parentheses; –: not determined. [b]Selectivity index: MDL_{50}/IC_{50} for *P. falciparum*.

DOI: 10.1021/acs.jnatprod.7b00876
J. Nat. Prod. XXXX, XXX, XXX−XXX

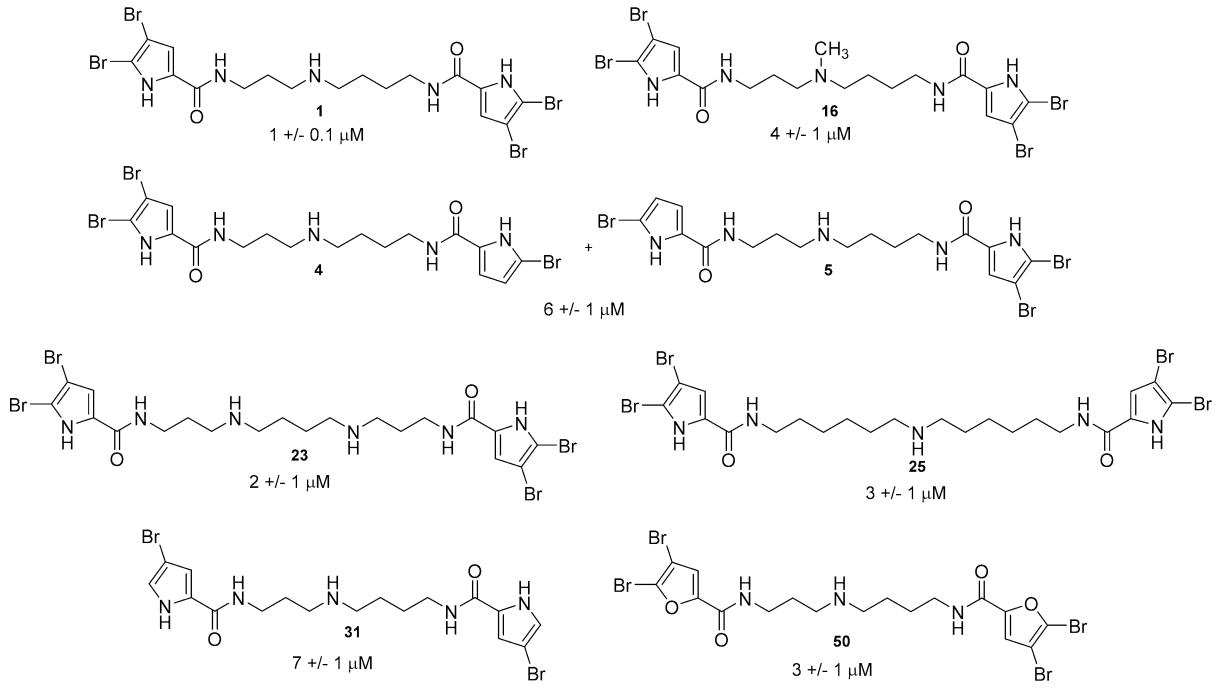

Figure 2. Structures and antiplasmodial activities of pseudoceratidine derivatives against *Plasmodium falciparum*.

N^1-(6-aminohexyl)hexane-1,6-diamine (**24**), in 60% and 68% yield, respectively. An additional variation introduced into the polyamine chain was introduction of a sulfur atom into the chain through synthesis of dialkyl sulfide **27** from 2-(2-aminoethylthio)ethanamine (**26**) and ketone **14** in a microwave reactor in 38% yield.

We also investigated changes in substituents on the pyrrole moieties while keeping the spermidine linker unchanged, with the exception of a nonbrominated derivative of **20**, namely, **28**, prepared in 60% yield by coupling of pyrrole ketone **13** and 1,5-diaminopentane (**18**). The spermidine-derived nonbrominated variant **29** was obtained in a similar manner in 70% yield. Monobromination of **13** at C-4 to provide **30** in 44% yield was achieved with 1-chloromethyl-4-fluor-1,4-diazoniabicyclo[2.2.2]octane bis(tetrafluoroborate) (Selectfluor, or F-TEDA-BF_4) in the presence of KBr.[39] Reaction of **30** with spermidine (**15**) under the same conditions for the synthesis of pseudoceratidine gave 2,21-debromopseudoceratidine (**31**) in 65% yield. Chlorination of **13** with sulfuryl chloride provided 2,2,2-trichloro-1-(4,5-dichloro-1*H*-pyrrol-2-yl)ethenone (**32**) in 15% yield. Coupling of **32** with spermidine led to the chlorinated version of pseudoceratidine (**33**) in 38% yield. Monofluorination at C-5 of **13** was achieved with Selectfluor in a microwave reactor at 70 °C to provide **34** in 20% yield.[40] Coupling of **34** with spermidine under basic conditions gave **35** in 65% yield.

More substantial changes in the aromatic moieties of pseudoceratidine were also introduced. Coupling of indole-2-carboxylic acid (**36**) and 1*H*-benzo[*d*]imidazole-2-carboxylic acid (**37**) with spermidine gave derivatives **38** and **39** in moderate yields. Coupling with 5-bromothiophene-2-carboxylic acid (**40**) and 5-methylthiophene-2-carboxylic acid (**41**) gave **42** and **43** in low yield. Reaction of 6-chloropyridine-2-carboxylic acid (**44**) or 6-methylpyridine-2-carboxylic acid (**45**) with spermidine provided the pyridine derivatives **46** and **47** also in low yield. Finally, the coupling of furan derivatives **48** and **49** with spermidine enabled us to obtain bis-furans **50** and **51** in moderate yields.

Antiparasitic Activity and SAR Investigation of Pseudoceratidine and Derivatives. Pseudoceratidine (**1**) was assayed against four protozoan parasite species: *P. falciparum*, *L.* (*L.*) *amazonensis* (etiological agent of localized and diffuse cutaneous leishmaniasis in South America), *L.* (*L.*) *infantum* (causative agent of visceral leishmaniasis in the Mediterranean and in Latin America), and *T. cruzi*. Although **1** was essentially inactive against *L.* (*L.*) *amazonensis*, *L.* (*L.*) *infantum*, and *T. cruzi*, it showed very good antiplasmodial activity (1.1 ± 0.1 μM) against *P. falciparum* (Table 5). The inseparable mixture of structural isomers 3-debromopseudoceratidine (**4**) and 20-debromopseudoceratidine (**5**) showed 5-fold decreased antiparasitic activity on *P. falciparum* (5.8 ± 0.5 μM), while *N*-acetylpseudoceratidine (**2**) did not display any antiparasitic activity. The isomeric pair of tedamides A (**9**) and B (**10**) was also inactive as antiparasitic agent. The preparation of pseudoceratidine derivatives **2**, **16**, **17**, **20**, **21**, **23**, **25**, **27**–**29**, **31**, **33**, **35**, **38**, **39**, **42**, **43**, **46**, **47**, **50**, and **51** in adequate amounts enabled us to explore the impact on bioactivity through variation of the pseudoceratidine polyamine chain and aromatic end groups. *N*-Methylpseudoceratidine (**16**) showed good antiplasmodial activity against *P. falciparum* (4 ± 1 μM). Compound **23**, with a larger polyamine chain bearing two basic nitrogens, showed antiplasmodial activity similar to that of the natural product (3 ± 1 μM), while compound **25**, with a polyamine chain of similar length but with only one basic nitrogen, displayed a 2-fold decrease in antiplasmodial activity (2 ± 1 μM). The 2,21-debromopseudoceratidine (**31**) derivative showed a decrease in antiplasmodial activity (7 ± 1 μM) relative to pseudoceratidine (**1**). Finally, the furan derivative **50**, bearing four bromine atoms, also showed good antiplasmodial activity against *P. falciparum* (3 ± 1 μM).

Although pseudoceratidine (**1**) was inactive against *L.* (*L.*) *infantum* promastigotes, derivatives **20**, **23**, **27**, **42**, and **50** showed enhanced, but yet moderate and similar, antileishma-

DOI: 10.1021/acs.jnatprod.7b00876
J. Nat. Prod. XXXX, XXX, XXX−XXX

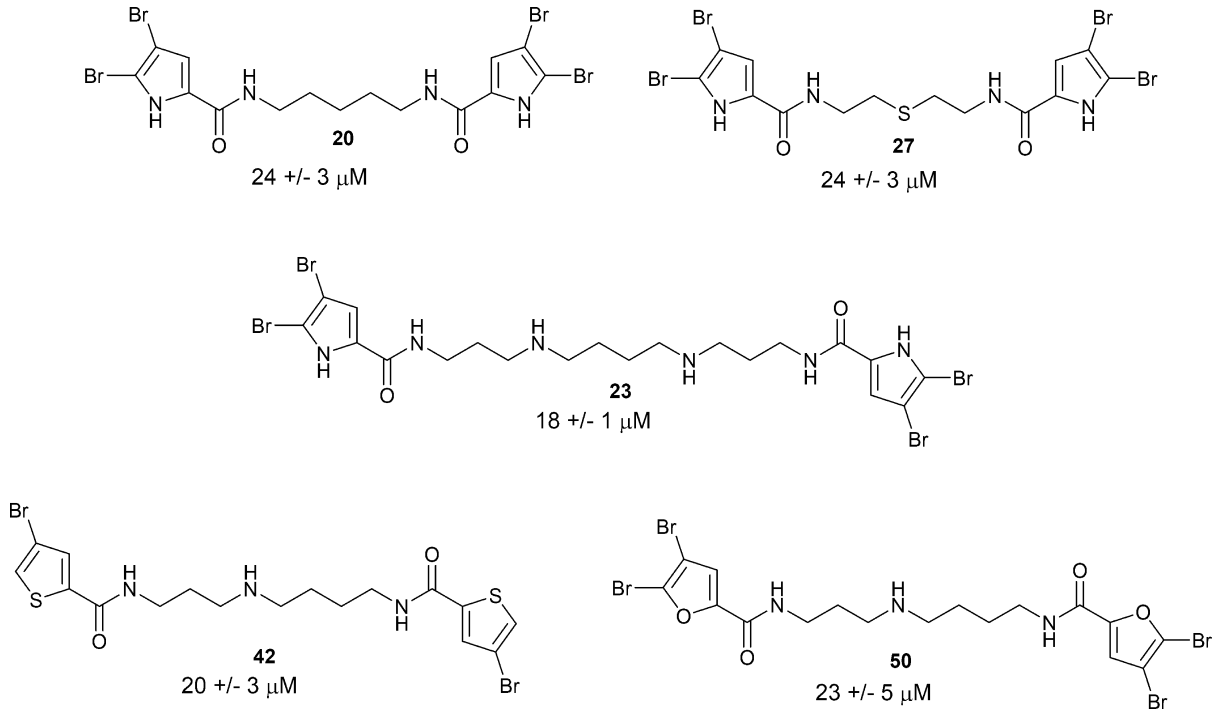

Figure 3. Structures and antileishmanial activities of pseudoceratidine derivatives against *Leishmania* (*L.*) *infantum*.

nial activity (EC_{50}s ~20 μM). The same derivatives were active, but considerably less potent, against *L.* (*L.*) *amazonensis*. Only compound **20** showed good antiparasitic activity against *T. cruzi* epimastigotes, while compound **27** showed weak activity in the same bioassay.

Leishmania and *Trypanosoma* species are Euglenozoa kinetoplastida parasites, while *P. falciparum* belongs to Hemosporida within the phylum Apicomplexa.[41] Constituting two groups of phylogenetically distant parasites, not surprisingly compounds affecting these two groups of organisms may show distinct effects. Our results indicated a selective, more potent activity against *P. falciparum* for compounds **1**, **4** and **5**, **16**, **23**, **25**, **31**, and **50** (Table 5 and Figure 2). It is evident the importance of bromine substituents in the aromatic extremities of pseudoceratidine derivatives for the antiplasmodial activity. Fully debrominated pseudoceratidine (**29**) is completely inactive, as well as the chlorinated derivative **33** and fluorinated **35**. Although methyl groups represent a structural variation similar to bromine groups in terms of van der Waals radii,[42] the bis-methylated bis-furan pseudoceratidine derivative **51** is completely inactive as well. Thus, bromination in both pyrrole and furan pseudoceratidine derivatives is essential for the expression of antiplasmodial activity against *P. falciparum*, which seems to be related to the electronic effect of bromine on aromatic rings rather than to its van der Waals radius or to an enhanced lipophilic character promoted by the bromine substituents.[43] The nature of the polyamine chain is an additional structural characteristic that determines the antiplasmodial activity of pseudoceratidine derivatives. Compounds **20** and **21**, which are devoid of a basic nitrogen, but have similar chain length (e.g., **21**) when compared to **1**, are inactive as antiplasmodial agents. The sulfur-bearing derivative **27** is inactive as well. On the other hand, compounds **23** and **25**, with longer polyamine chains, are as active as pseudoceratidine (**1**). The *N*-methyl derivative **16** is still active, but approximately 4-fold less active than pseudoceratidine. Therefore, a basic linker in the form of the polyamine chain appears important for antiplasmodial activity.

Derivatives with an *N*-acyl group (**2** and **17**) are inactive against *P. falciparum*, suggesting the importance of the basic nitrogens in the polyamine chain. These compounds were also inactive against *Leishmania* species and *T. cruzi* tested in our assays, which prevents simple acylation of pseudoceratidine to access cellular probes. However, alkylation of pseudoceratidine derivatives was tolerated since they maintain the basic nitrogen atom. The selectivity index of the antiplasmodial activity of compounds **1**, **4**, **5**, **16**, **23**, **25**, **31**, and **50** was determined by measuring cytotoxicity on the human liver cancer HepG2 cell line (Table 5). Pseudoceratidine (**1**) was the most cytotoxic compound (16 ± 1 μM), but with a selectivity index of 15. Compounds **16**, **4**, **5**, **23**, **25**, **31**, and **50** displayed overall weak cytotoxicity, with selectivity indices between 35 and 125, which are considered excellent, as this shows dramatically reduced toxicity to healthy cells.

As for the anti-Leishmanial activity, compounds **20**, **23**, **27**, **42**, and **50** are moderate to weakly active (EC_{50} in the range between 19 and 24 μM; Figure 3). However, a clear picture of the structural requirements for anti-Leishmanial activity of these pseudoceratidine derivatives did not emerge. Compounds **20** and **27** have shorter polyamine chains devoid of a basic nitrogen, but the opposite is true for compounds **23**, **42**, and **50**. Bromination seems to be important, but the nature of the aromatic ring is apparently less relevant for the antileishmanial activity. Therefore, further variations on this series of antileishmanial compounds need to be explored in order to clarify structure−activity relationships aiming to improve the effectiveness of toxicity toward *L.* (*L.*) *infantum* promastigotes.

In vitro infections were performed aiming to evaluate the activity of compounds **23**, **42**, and **50** against *Leishmania* intracellular amastigotes. Because amastigotes must reside inside macrophages, we first determined the cytotoxicity of

DOI: 10.1021/acs.jnatprod.7b00876
J. Nat. Prod. XXXX, XXX, XXX−XXX

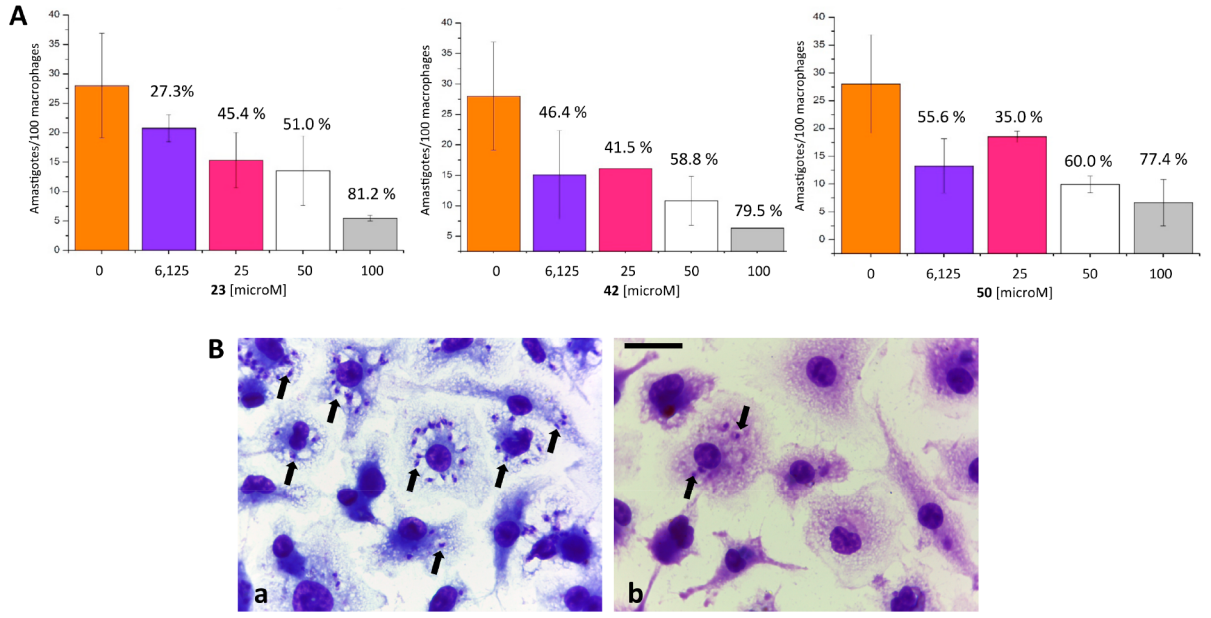

Figure 4. *In vitro* activity of **23**, **42**, and **50** against intracellular *Leishmania* (*L.*) *amazonensis* amastigotes. Macrophages derived from BALB/c mice bone marrow were infected with *L.* (*L.*) *amazonensis* stationary promastigotes for 1 h (MOI = 10). After 24 h, infected cells were incubated with 6.125, 25, 50, or 100 μM of each compound for 24 h. MeOH-fixed cells were stained, and infection was determined by counting 300 cells/coverslip. Experiments were performed in triplicate. The results shown are representative of two independent experiments. (A) Bars indicate the number of intracellular amastigotes. Numbers above each bar indicate the percentage of reduction over control untreated infected macrophages. (B) Photomicrograph examples showing untreated infected macrophages (a) and infected macrophages incubated with compound **42** at 100 μM (b). Arrows point to intracellular amastigotes. Bar = 10 μm.

active pseudoceratidine derivatives against bone-marrow-derived macrophages from BALB/c mice. Compounds **23** and **42** showed low toxicity (CC_{50} > 100 μM). The half-maximal cytotoxic concentration for compound **50** was 83 ± 4 μM. Compounds **23**, **42**, and **50** were selected for further investigation of their activities on intracellular amastigotes. Bone-marrow-derived macrophages were infected with *L.* (*L.*) *amazonensis* stationary phase promastigotes (MOI = 10) for 24 h and then incubated with increasing concentrations of compounds **23**, **42**, and **50** for subsequent counting of intracellular amastigotes. Intracellular parasitism was reduced in a dose-dependent manner after 24 h for **23**, **42**, and **50** (Figure 4), leading to approximately 80% reduction of the amastigote number over the control group at higher concentrations. The intracellular effect against *Leishmania* amastigotes was almost equivalent when comparing compounds **23**, **42**, and **50**. Further studies should evaluate the effects of compounds **23**, **42**, and **50** in experimental leishmaniasis.

In order to better characterize the antiplasmodial activity of pseudoceratidine (**1**), the most active compound against *P. falciparum*, its impact on the morphology of HepG2 cells was evaluated after 24 h of parasite treatment at a concentration 10-fold higher than its IC_{50} value on the parasites. Pseudoceratidine (**1**) was not toxic to HepG2 cells at this high concentration, as HepG2 cells showed microscopic morphology similar to untreated cells. Pseudoceratidine (**1**) was then tested against multiresistant *P. falciparum* strain (K1 strain) and still presented very good potency against this K1 resistant strain, with an IC_{50} value of 1.1 ± 0.1 μM (Figure 5 and Table 6).

Aiming to assess the stage-specific inhibitory activity of pseudoceratidine (**1**), it was incubated at a concentration 10-fold higher than IC_{50} values with highly synchronized parasites.

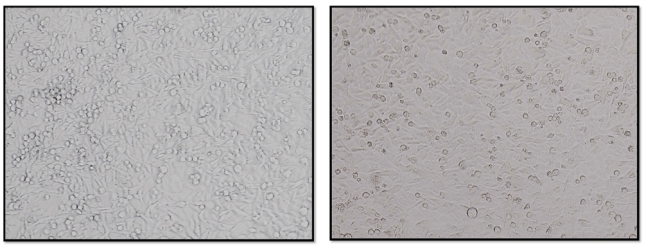

Figure 5. HepG2 cell morphology before (left) and after (right) treatment with pseudoceratidine (**1**) at 10 μM.

Table 6. Antiplasmodial Activities of Pseudoceratidine (1) and Standard Antimalarials against Sensitive (3D7 Strain) and Resistant *Plasmodium falciparum* (K1 Strain)

	P. falciparum IC_{50} (μM)	
compound	3d7 strain	K1 strain
pseudoceratidine (**1**)	1.1 ± 0.1	1.1 ± 0.1
chloroquine	0.013 ± 0.002	0.167 ± 0.002
pyrimethamine	0.03 ± 0.01	3.9 ± 0.1
cycloguanil	0.010 ± 0.002	0.54 ± 0.02
artesunate	0.004 ± 0.001	0.003 ± 0.001

Cell morphological changes were observed by microscopy at 0, 8, 16, and 32 h postsynchronization (Figure 6). Pseudoceratidine (**1**) showed inhibitory activity in the early ring stages, inducing alterations in *P. falciparum* morphology between 8 and 16 h after incubation. These data suggest a fast-acting mechanism in which young forms of *P. falciparum* in the intraerythrocytic cycle are highly susceptible to the antiparasitic activity of **1**. The potential drug interactions of pseudoceratidine (**1**) with sodium artesunate against *P. falciparum* were also assayed, in order to elucidate potential

DOI: 10.1021/acs.jnatprod.7b00876
J. Nat. Prod. XXXX, XXX, XXX−XXX

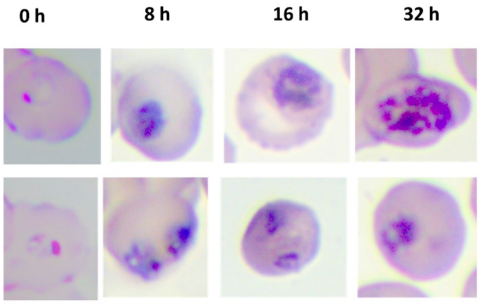

Figure 6. Microscopy of synchronized parasites continuously treated with pseudoceratidine (**1**) at a concentration 10-fold the IC_{50} value (top line) and DMSO (control, bottom line). Images are representative of three independent experiments.

benefits and limitations of candidate molecules in combination with antimalarial drugs.[44] The isobologram analysis and FIC index (1.0 ± 0.2) indicate an additive interaction effect of pseudoceratidine (**1**) in combination with artesunate, thereby suggesting that pseudoceratidine derivatives may be used in artemisinin-based combination therapies (Figure 7).

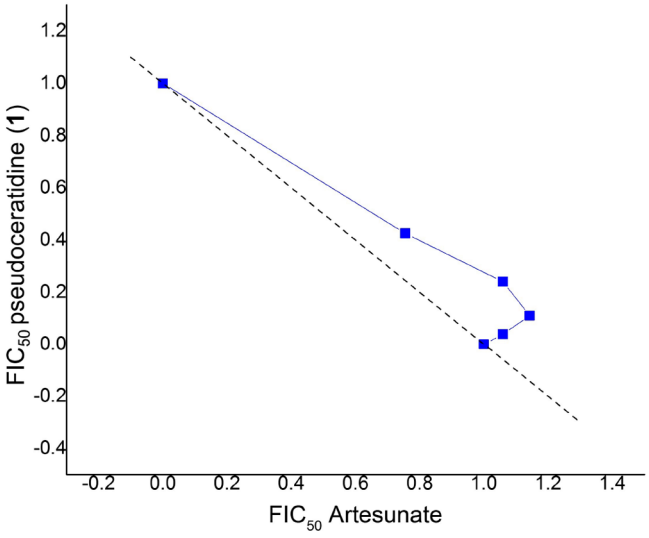

Figure 7. Isobologram plot for drug interaction analysis of pseudoceratidine (**1**) and sodium artesunate.

Bromopyrrole alkaloids related to oroidin have been assayed against a series of parasites. Dispacamide B, spongiacidin B, and dibromopalau'amine displayed antiplasmodial activity against *P. falciparum* comparable to that of pseudoceratidine (1.34, 1.09, and 1.48 mg/mL, respectively).[45] Dibromopalau'amine was also very active against *T. brucei rhodesiense* (0.46 μg/mL) and against *L. donovani* (1.48 μg/mL). Longamide B also showed good antiparasitic activity against *T. brucei rhodesiense* (1.53 μg/mL) and against *L. donovani* (3.85 μg/mL).[45] Oroidin showed good antiparasitic activity against *P. falciparum* (3.9 μg/mL) and moderate activity against *T. brucei rhodesiense* (17.3 μg/mL), being inactive against *L. donovani* and *T. cruzi*.[46] Simpler derivatives 4,5-dibromo-1*H*-pyrrole-2-carboxylic acid and the respective methyl ester showed better antiplasmodial activity (5.8 and 7.9 μg/mL, respectively).[46] It is clear that a detailed investigation of bromopyrrole alkaloids as antiparasitic agents, particularly as antiplasmodial compounds, is a worthy area for further research.

CONCLUSION

In the present investigation, we report the isolation of eight new pseudoceratidine derivatives from the sponge *T. brasiliensis*, of which the tedamides encompass a new 4-bromo-4-methoxy-5-oxo-4,5-dihydro-1*H*-pyrrole-2-carboxamide moiety. Pseudoceratidine displayed very good antimalarial activity and justified the preparation of 23 of its derivatives, aiming to establish initial structure−activity relationships. Pseudoceratidine and seven synthetic derivatives indicated that the length of the polyamine chain bearing a basic nitrogen and the presence of bromine atoms on pyrrole or furan terminal moieties represent essential structural features for the expression of antiplasmodial activity. Pseudoceratidine (**1**) showed antiplasmodial activity against both sensitive (3D7 strain) and resistant (K1 strain) *P. falciparum* strains and also an additive interaction effect in combination with artesunate, indicating that derivatives of **1** may be used in combination with artemisinin for the treatment of malaria. The results described demonstrate that the pseudoceratidine scaffold, which is easily obtained by total synthesis, constitutes a useful lead to be developed as potential antiplasmodial agents.

EXPERIMENTAL SECTION

General Experimental Procedures. UV spectra were recorded on a Shimadzu UV-3600 spectrophotometer. IR spectra were obtained on a Shimadzu IRAffinity-1 Fourier transform infrared spectrophotometer on a silica plate. NMR spectra were obtained at 25 °C, with tetramethylsilane as an internal standard, using a Bruker ARX 9.4 T spectrometer operating at either 400.35 MHz (^{1}H) or 100.10 MHz (^{13}C) and a Bruker AV-600 spectrometer operating at either 600 MHz (^{1}H) or 150 MHz (^{13}C) with a 2.5 mm cryoprobe. The ^{1}H chemical shifts are referenced to the residual DMSO-d_6 (δ 2.49), whereas ^{13}C chemical shifts are referenced to the DMSO-d_6 solvent peaks (δ 39.5). HRMS and direct insertion MS/MS analyses were performed on a Waters Xevo QTOF MS/MS instrument using the following conditions: capillary voltage, 1.20 kV; desolvation temperature, 450 °C; voltage cone, 30 V; electrospray, positive mode; detection range, 100−1000 Da with total ion count extracting acquisition. Cone and desolvation gas flows were set to 700 L h^{-1}, respectively, with a nitrogen source. HPLC semipreparative and preparative separations were performed with a Waters instrument (600 quaternary pump and 2487 double-beam UV detector), with 0.1% formic acid in all eluents utilized. HPLC-UV-ELSD-MS analyses were performed using a Waters Alliance 2695 instrument coupled online with a Waters 2996 photodiode array detector and a Waters 2424 evaporative light-scattering detector, followed by a Micromass ZQ 2000 detector with an electrospray interface. The mass spectrometer detector was optimized using the following conditions: capillary voltage, 3.00 kV; source block temperature, 100 °C; desolvation temperature, 350 °C; voltage cone, 25 V; electrospray, positive mode; detection range, 200−900 Da with total ion count extracting acquisition. Cone and desolvation gas flows were set to 50 and 350 L h^{-1}, respectively, with a nitrogen source.

Animal Material. The sponge *Tedania brasiliensis* was collected at Cabo Frio (Rio de Janeiro state, in April 2011) and identified by one of the authors (E.H.). A voucher of the collected sponge has been deposited at the Museu Nacional do Rio de Janeiro, Universidade Federal do Rio de Janeiro (MNRJ 16876).

Extraction and Isolation. A 136.2 g freeze-dried sample of *T. brasiliensis* was homogenized and exhaustively extracted with 5 L of MeOH. The solvent was evaporated to 500 mL. The resulting MeOH extract was diluted with 50 mL of H_2O and partitioned with hexane (3 × 500 mL). The MeOH/H_2O fraction was evaporated to dryness and dissolved in 1 L of 1:1 EtOAc/H_2O. Partitioning was performed two additional times. The EtOAc fraction was evaporated to dryness to yield 5.37 g. The hexane extract was also evaporated to dryness to yield 1.79 g of an apolar fraction. The aqueous fraction of the EtOAc/

DOI: 10.1021/acs.jnatprod.7b00876
J. Nat. Prod. XXXX, XXX, XXX−XXX

H_2O partition was extracted with a 1:1 mixture of XAD-4 and XAD-7, after which the resins were desorbed with MeOH, then with 1:1 MeOH/acetone, and the organic solvents were evaporated to dryness. Antiparasitic assays performed with the hexanes, EtOAc, and resin-extracted H_2O fractions indicated bioactivity exclusively in the EtOAc fraction. HPLC-UV-MS analysis of these three fractions indicated pseudoceratidine (**1**) and its minor derivatives only in the EtOAc fraction as well. Therefore, neither the hexanes nor resin-extracted H_2O fractions were investigated.

The EtOAc fraction (5.37 g) was subjected to solid-phase extraction on a C_{18} reversed-phase cartridge (Waters) eluted with a gradient of MeOH in H_2O. After their evaporation and TLC analysis, the fractions obtained were pooled into eight fractions, named TBA1 (608 mg), TBA2 (567 mg), TBA3 (347 mg), TBA4 (377 mg), TBA5 (251 mg), TBA6 (383 mg), TBA7 (338 mg), and TBA8 (399 mg). Fraction TBA2 was separated by HPLC using an Inertsil ODS-2 column (250 × 9.4 mm, 5 μm), with a H_2O/MeCN ratio of 75:25, a flow rate of 1.5 mL/min, and detection performed at λ_{max} 254 nm. Six fractions were obtained, among which fraction TBA2B (42.1 mg) was further investigated and fraction TBA2F (28.1 mg) was identified as 4,5-dibromo-1*H*-pyrrole-2-carboxylic acid. Fraction TBA2B was separated by HPLC using an Inertsil ODS-2 column (250 × 9.4 mm, 5 μm), with a H_2O/MeCN ratio of 67:33, a flow rate of 1.5 mL/min, and detection performed at λ_{max} 254 nm. Seven fractions were obtained, among which fraction TBA2B3 (9.4 mg) was identified as a mixture of tedamides A (**9**) and B (**10**), fraction TBA2B5 (1.3 mg) was identified as 3-debromopseudoceratidine (**4**) and 20-debromopseudoceratidine (**5**), and fraction TBA2B7 (10.2 mg) was identified as pseudoceratidine (**1**).[8]

HPLC separation of fraction TBA3 using an Inertsil ODS-2 column (250 × 9.4 mm, 5 μm), with a gradient of MeOH in H_2O from 40% MeOH to 100% MeOH over 45 min (flow rate of 1.5 mL/min and detection at λ_{max} 254 nm), yielded six fractions, among which fraction TBA3-4 (71.8 mg) was identified as pure pseudoceratidine (**1**) and fractions TBA3-3 (17.0 mg), TBA3-5 (13.3 mg), and TBA3-6 (4.3 mg) were further investigated. Fraction TBA3-3 was separated using an Inertsil ODS-3 column (250 × 4.6 mm, 5 μm), with a gradient of MeOH in H_2O from 38% MeOH to 60% MeOH over 38 min (flow rate of 1.0 mL/min and detection at λ_{max} 254 nm), to yield six fractions, among which TBA3-3C (2.3 mg) was identified as a mixture of tedamides C (**11**) and D (**12**). Fraction TBA3-5 (13.3 mg) was separated by HPLC using an Inertsil ODS-3 column (250 × 4.6 mm, 5 μm), with a gradient of MeOH in H_2O from 10% MeOH to 100% MeOH over 35 min (flow rate of 1.0 mL/min and detection at λ_{max} 254 nm), to yield four fractions, among which fraction TBA3-5B (2.7 mg) was further purified using an Inertsil ODS-3 column (250 × 4.6 mm, 5 μm), with a gradient of MeOH in H_2O from 55% MeOH to 60% MeOH over 30 min (flow rate of 1.0 mL/min and detection at λ_{max} 254 nm), to yield pure 19-bromopseudoceratidine (**7**) (1.0 mg). Fraction TBA3-6 (4.3 mg) was purified by HPLC using an Inertsil ODS-3 column (250 × 4.6 mm, 5 μm), with a gradient of MeOH in H_2O from 10% MeOH to 100% MeOH over 35 min (flow rate of 1.0 mL/min and detection at λ_{max} 254 nm), to yield 0.5 mg of 4,19-dibromopseudoceratidine (**8**).

Separation of fraction TBA-5 (250.5 mg) by HPLC using an Inertsil ODS-2 column (250 × 9.4 mm, 5 μm) and a gradient of 1:1 MeOH/MeCN in H_2O, from 44% to 100% of the organic mixture over 30 min, yielded seven fractions, among which TBA-5D (80.7 mg) was identified as pure pseudoceratidine (**1**).

Separation of the fraction TBA-7 (338 mg) by HPLC using an Inertsil ODS-2 column (250 × 9.4 mm, 5 μm), with a gradient of MeOH/MeCN (1:1) in H_2O from 44% MeOH to 100% MeOH/MeCN (1:1) over 35 min (flow rate of 1.5 mL/min and detection at λ_{max} 254 nm), yielded fraction TBA-7A (98.2 mg). This fraction was further separated by HPLC using an Inertsil ODS-3 column (250 × 4.6 mm, 5 μm), with a gradient of MeOH/MeCN (1:1) in H_2O from 30% to 100% MeOH/MeCN (1:1) over 30 min (flow rate of 1.0 mL/min and detection at λ_{max} 254 nm), to yield 10 fractions, among which TBA-7A8 (5.0 mg) was identified as a mixture of 4-bromopseudoceratidine (**6**) and 19-debromopseudoceratidine (**7**).

*3-Debromopseudoceratidine (**4**) and 20-debromopseudoceratidine (**5**):* colorless, glassy solid; UV (MeOH) λ_{max} (log ε) 215 (4.2), 235 (4.2), 274 (4.6) nm; IR (film) ν_{max} 3186, 2945, 1677, 1629, 1133, 740, and 615 cm^{-1}; ^1H and ^{13}C NMR data, Tables 1 and 2; HRESIMS *m/z* 565.9409 $[M + H]^+$ (calcd for $C_{17}H_{23}{}^{79}Br_3N_5O_2$, 565.9402).

*4-Bromopseudoceratidine (**6**) and 19-bromopseudoceratidine (**7**):* colorless, glassy solid; UV (MeOH) λ_{max} (log ε) 215 (4.2), 235 (4.2), 277 (4.6) nm; ^1H and ^{13}C NMR data, Tables 1 and 2; HRESIMS *m/z* 721.7632 $[M + H]^+$ (calcd for $C_{17}H_{21}{}^{79}Br_5N_5O_2$, 721.7612).

*4,19-Dibromopseudoceratidine (**8**):* glassy solid; UV (MeOH) λ_{max} (log ε) 222 (4.2), 235 (4.2), 274 (4.6) nm; ^1H and ^{13}C NMR data, Tables 1 and 2; HRESIMS *m/z* 799.6749 $[M + H]^+$ (calcd for $C_{17}H_{20}{}^{79}Br_6N_5O_2$, 799.6717).

*Tedamide A (**9**) and tedamide B (**10**):* colorless, glassy solid; $[\alpha]_D$ −7.75 (*c* 0.007, MeOH); UV (MeOH) λ_{max} (log ε) 218 (4.2), 275 (4.2) nm; IR (film) ν_{max} 3103, 2938, 2842, 1718, 1677, 1526, 1202, 1139, and 719 cm^{-1}; ^1H and ^{13}C NMR data, Tables 3 and 4; HRESIMS *m/z* 611.9452 $[M + H]^+$ (calcd for $C_{18}H_{25}{}^{79}Br_3N_5O_4$, 611.9456).

*Tedamide C (**11**) and tedamide D (**12**):* colorless, glassy solid; $[\alpha]_D$ +107.33 (*c* 0.0006, MeOH); UV (MeOH) λ_{max} (log ε) 218 (4.2), 275 (4.2) nm; ^1H and ^{13}C NMR data, Tables 3 and 4; HRESIMS *m/z* 689.8571 $[M + H]^+$ (calcd for $C_{18}H_{24}{}^{79}Br_4N_5O_4$, 689.8562).

Preparation of N^{12}-Acetylpseudoceratidine (2) and N^{12}-Formylpseudoceratidine (3). Pseudoceratidine (**1**, 5.0 mg, 7.7 mM) was dissolved in freshly distilled pyridine (1 mL), and acetic anhydride (1 mL, 10.6 mM) was added. The reaction was left under magnetic stirring for 60 h, after which the pyridine/Ac_2O mixture was evaporated *in vacuo*. The reaction mixture was purified by HPLC using an Inertsil ODS-3 column (250 × 4.6 mm, 5 μm), with 65% MeOH, a flow rate of 1.0 mL/min, and detection performed at λ_{max} 254 nm. N^{12}-Acetylpseudoceratidine (**2**) (2.7 mg) and N^{12}-formylpseudoceratidine (**3**) (1.4 mg) were obtained in 50.7% and 26.9% yields, respectively.

*N^{12}-Acetylpseudoceratidine (**2**):* colorless, glassy solid; UV (MeOH) λ_{max} (log ε) 222 (4.2), 235 (4.2), 275 (4.6) nm; IR (film) ν_{max} 2924, 2842, 1608, 1560, 1526, and 664 cm^{-1}; ^1H and ^{13}C NMR data, Tables 1 and 2; HRESIMS *m/z* 683.8433 $[M - H]^-$ (calcd for $C_{19}H_{22}{}^{79}Br_4N_5O_3$, 683.8456).

*N^{12}-Formylpseudoceratidine (**3**):* colorless, glassy solid; UV (MeOH) λ_{max} (log ε) 222 (4.2), 235 (4.2), 275 (4.6) nm; IR (film) ν_{max} 2924, 2842, 1587, 1360, and 650 cm^{-1}; ^1H and ^{13}C NMR data, Tables 1 and 2; HRESIMS *m/z* 669.8283 $[M - H]^-$ (calcd. for $C_{18}H_{22}{}^{79}Br_4N_5O_3$, 671.8299).

Bioassay Procedures. *Chemical Compounds.* Alamar blue (resazurin), DMSO, MeOH, M-199 medium, RPMI-1640, phosphate-buffered saline (PBS), sodium azide (99.5% purity), bacterial lipopolysaccharide (99% purity), TritonX-100 (99% purity), and benznidazole (97% purity) were purchased from commercial suppliers.

Anti-Leishmanial and Anti-Trypanosoma cruzi in Vitro Assays. *L.* (*L.*) *amazonensis* (MHOM/BR/1973/M2269) promastigotes were maintained at 26 °C in Medium 199 (Sigma-Aldrich) supplemented with 5% penicillin/streptomycin, 0.1% hemin (25 mg/mL in 50% triethanolamine), 20% heat-inactivated fetal bovine serum, 10 mM adenine (pH 7.5), and 5 mM L-glutamine.[47] *L.* (*L.*) *infantum* (MHOM/BR/1972/LD) was cultured as described above, with the exception that 5% human sterile urine was added to the culture medium. *T. cruzi* epimastigotes (Y strain) were grown in liver infusion tryptose medium supplemented with 20 mg/L hemin and 10% fetal calf serum at 28 °C as previously described.[48] The antiparasitic activity of pseudoceratidine derivatives was assessed against trypanosomatids, using an MTT viability assay[49] after 24 h of incubation with the series of pseudoceratidine derivatives. The half-maximal effective concentration (EC_{50}) values for the *Leishmania* spp. and *T. cruzi* populations were calculated from sigmoidal regression of the concentration−response curves using Scientific Graphing and

DOI: 10.1021/acs.jnatprod.7b00876
J. Nat. Prod. XXXX, XXX, XXX−XXX

Analysis Software Origin 5.0. Each experiment was performed in triplicate and repeated two or three times. Cytotoxic experiments were conducted using bone marrow macrophages from BALB/c female mice. Differentiated cells were cultured in 96-well plates at 37 °C for posterior incubation with increasing concentrations of pseudoceratidine derivatives for 24 h. The MTT method was also performed, and CC_{50} values were calculated accordingly.[49]

Intracellular infections were obtained by infecting bone-marrow-derived macrophages with stationary phase *L.* (*L.*) *amazonensis* promastigotes (10 parasites: 1 macrophage; MOI = 10). After 1 h of incubation with the parasites, cultures were washed three times with PBS 1× and maintained at 33 °C, 5% CO_2, for 24 h. After this period, infections were established and different concentrations of pseudoceratidine compounds were added to the cultures, which remained at 33 °C for 24 h. Cells were then washed three times with warm PBS 1× and fixed with MeOH for subsequent staining using the Instant Prov kit (Newprov). The number of intracellular amastigotes was obtained by counting 300 cells in triplicate coverslips. Photomicrographs of infections were recorded using the Leica LAS Core microscope system. Experiments using BALB/c mice were approved by the Ethical Committee for Animal Experimentation of the Biology Institute of the State University of Campinas−UNICAMP (4535-1/2017).

Antiplasmodial in Vitro Assays against P. falciparum Blood Parasites. *P. falciparum* blood parasites [3D7, sensitive strain; K1, chloroquine-, cycloguanil-, and pyrimethamine-resistant strain] were cultured as previously described.[50] Freshly sorbitol synchronized ring stages[51] were incubated with the test samples at various concentrations, previously solubilized in 0.05% DMSO (v/v). Each assay was performed in triplicate. Results were compared with control cultures in complete medium with no assay samples. Pyrimethamine, chloroquine, cycloguanil, and sodium artesunate were used in each experiment as antimalarial controls. The activity of test samples was measured using the SYBR green assay.[52] Briefly, the plates were centrifuged at 700*g* for 5 min at room temperature to remove the medium, washed with 1× PBS, and incubated for 30 min with lysis buffer solution [2.4228 g of TRIS, ultrapure (for 20 mM solution), pH 7.5; 1.8612 g of EDTA 5 mM ultrapure (for 5 mM solution); 80 μg of saponin (0.008% w/v); 800 μL of Triton X-100 (0.08% v/v); H_2O Type I] and SYBR green I DNA stain (1:20 000). The fluorescence of uninfected erythrocytes was considered as a background. Fluorescence was measured on a SpectraMax340PC384 fluorimeter at 485/535 nm. The half-maximal compound inhibitory concentration (IC_{50}) was estimated by curve fitting using software from the OriginLab Corporation and comparing to the parasite growth in test-sample-free medium.

Cytotoxicity Tests Using Immortalized Cells. The cytotoxicity of test compounds was evaluated in a human hepatoma cell line (HepG2) using cells cultured in 75 cm^2 sterile flasks containing RPMI-1640 medium (supplemented with 10% heat-inactivated fetal bovine serum and 40 mg/L gentamicin) under a 5% CO_2 atmosphere at 37 °C. When confluent, the cell monolayer was washed with culture medium, trypsinized, distributed in a flat-bottomed 96-well plate (5×10^3 cells/well), and incubated for 18 h at 37 °C for cell adherence.[53] The compounds (in 20 μL of solution) at various concentrations (1000−1 μg/mL) were placed in 96-well plates and incubated with the cultured cells for 24 h under a 5% CO_2 atmosphere at 37 °C. Then, 3-(4,5-dimethylthiazol-2-yl)-2,5-diphenyltetrazolium bromide (MTT) solution (5 mg/mL; 20 μL/well for 3 h) was used to evaluate the mitochondrial viability. The supernatants were carefully removed, and 100 μL of DMSO was added to each well and mixed to solubilize the formazan crystals. The optical density was determined at 570 and 630 nm. The cell viability was expressed as the percentage of the control absorbance in the untreated cells after subtracting the appropriate background.

In Vitro Association with Artesunate. The isobologram was built to analyze the effects of drug combination aiming to determine the additive, synergic, or antagonistic effect. Briefly, the fractional half-maximum inhibitory concentration (FIC_{50}) was calculated for each drug pair combination. A stock drug solution was prepared for each drug using complete media, such that the final concentration approximates IC_{50} following three or four 2-fold dilutions. Using these stock solutions, volume−volume (v/v) mixtures of artesunate and pseudoceratidine (**1**) were prepared in 0:5, 1:4, 2:3, 1:4, and 5:0 ratios. These mixtures were 2-fold serially diluted to generate a range of seven concentrations in each case. The $\sum FIC_{50}$ were calculated using the following equation: FIC_{50} artesunate (IC_{50} of artesunate when combined with pseudoceratidine/artesunate IC_{50}) + FIC_{50} pseudoceratidine (IC_{50} of pseudoceratidine when combined with artesunate/pseudoceratidine IC_{50}). Isobologram curves were constructed by plotting FIC_{50} pseudoceratidine vs FIC_{50} artesunate. A straight diagonal line ($\sum FIC_{50} = 1$) indicates an additive effect between artesunate and pseudoceratidine, a concave curve below the diagonal ($FIC_{index} < 1$) indicates a synergistic effect, and a convex curve above the diagonal ($FIC_{index} > 1$) indicates antagonism.[54]

■ ASSOCIATED CONTENT

Supporting Information

The Supporting Information is available free of charge on the ACS Publications website at DOI: 10.1021/acs.jnatprod.7b00876.

Isolation procedures, HRMS, IR, and ^1H and ^{13}C NMR spectra of compounds **1**−**12**, synthesis procedures and IR, HRMS, and ^1H and ^{13}C NMR spectra of compounds **16**, **17**, **20**, **21**, **23**, **25**, **27**−**29**, **31**, **33**, **35**, **38**, **39**, **42**, **43**, **46**, **47**, **50**, and **51** (PDF)

■ AUTHOR INFORMATION

Corresponding Author

*Tel: +55-16-33739954. Fax: +55-16-33739952. E-mail: rgsberlinck@iqsc.usp.br.

ORCID

Daniel Romo: 0000-0003-3805-092X

Roberto G. S. Berlinck: 0000-0003-0118-2523

Present Address

‡Departamento de Química, Universidad Santiago de Cali, Calle 5#62-00, Santiago de Cali, Valle del Cauca, Colombia.

Author Contributions

#L. L. L. Parra and A. F. Bertonha contributed equally.

Notes

The authors declare no competing financial interest.

■ ACKNOWLEDGMENTS

The authors thank Dr. H. Xue (Baylor University) for help in the characterization of some of the synthetic derivatives and Dr. D. E. Williams (Department of Earth, Ocean and Atmospheric Sciences, University of British Columbia), for his assistance in some of the HRMS measurements. Financial support was provided by a FAPESP BIOTA/BIOprospecTA grant (2013/50228-8) awarded to R.G.S.B., CEPID-CIBFar grant (2013/07600-3) to G.O., CNPq (grants 471509/2012-4 and 405330/2016-2) to R.V.C.G., FAPESP Young Investigators Grant (2014/21129-4) to D.C.M., and a FAPESP Regular Research Grant (2015/24595-9) to F.R.G. L.L.L.P. and A.F.B. thanks CAPES for a Ph.D. scholarship and also for a Science without Borders scholarship at Baylor University for A.F.B.

■ REFERENCES

(1) Blunt, J. W.; Copp, B. R.; Keyzers, R. A.; Munro, M. H. G.; Prinsep, M. R. *Nat. Prod. Rep.* **2017**, *34*, 235−294 and previous reviews in this series.

DOI: 10.1021/acs.jnatprod.7b00876
J. Nat. Prod. XXXX, XXX, XXX−XXX

(2) Wang, X.; Ma, Z.; Wang, X.; De, S.; Ma, Y.; Chen, C. *Chem. Commun.* **2014**, *50*, 8628−8639.
(3) Al-Mourabit, A.; Zancanella, M. A.; Tilvic, S.; Romo, D. *Nat. Prod. Rep.* **2011**, *28*, 1229−1260.
(4) Braekman, J. C.; Daloze, D.; Stoller, C.; van Soest, R. W. M. *Biochem. Syst. Ecol.* **1992**, *20*, 417−431.
(5) van Soest, R. W. M.; Braekman, J. C. *Mem. Queensland Mus.* **1999**, *44*, 569−589.
(6) Erpenbeck, D.; van Soest, R. W. M. *Mar. Biotechnol.* **2007**, *9*, 2−19.
(7) Cárdenas, P.; Pérez, T.; Boury-Esnault, N. *Adv. Mar. Biol.* **2012**, *61*, 79−209.
(8) Tsukamoto, S.; Kato, H.; Hirota, H.; Fusetani, N. *Tetrahedron Lett.* **1996**, *37*, 1439−1440.
(9) Tsukamoto, S.; Kato, H.; Hirota, H.; Fusetani, N. *Tetrahedron* **1996**, *52*, 8181−8186.
(10) Ponasik, J. A.; Kassab, D. J.; Ganem, B. *Tetrahedron Lett.* **1996**, *37*, 6041−6044.
(11) Behrens, C.; Christoffersen, M. W.; Gram, L.; Nielsen, P. H. *Bioorg. Med. Chem. Lett.* **1997**, *7*, 321−326.
(12) Ariey, F.; Witkowski, B.; Amaratunga, C.; Beghain, J.; Langlois, A.-C.; Khim, N.; Kim, S.; Duru, V.; Bouchier, C.; Ma, L.; Lim, P.; Leang, R.; Duong, S.; Sreng, S.; Suon, S.; Chuor, C. M.; Bout, D. M.; Ménard, S.; Rogers, W. O.; Genton, B.; Fandeur, T.; Miotto, O.; Ringwald, P.; Le Bras, J.; Berry, A.; Barale, J. C.; Fairhurst, R. M.; Benoit-Vical, F.; Mercereau-Puijalon, O.; Ménard, D. *Nature* **2014**, *505*, 50−55.
(13) www.who.int/leishmaniasis/en/; World Health Organization, 2016. Accessed August, 2107.
(14) Kedzierski, L.; Sakthianandeswaren, A.; Curtis, J. M.; Andrews, P. C.; Junk, P. C.; Kedzierska, K. *Curr. Med. Chem.* **2009**, *16*, 599−614.
(15) Croft, S. L.; Olliaro, P. *Clin. Microbiol. Infect.* **2011**, *17*, 1478−83.
(16) Tempone, A. G.; Sartorelli, P.; Mady, C.; Fernandes, F. *Cardiovasc. Hematol. Agents Med. Chem.* **2007**, *5*, 222−235.
(17) Gascon, J.; Bern, C.; Pinazo, M. J. *Acta Trop.* **2010**, *115*, 22−27.
(18) Schmunis, G. A.; Yadon, Z. E. *Acta Trop.* **2010**, *115*, 14−21.
(19) Globalization and infectious diseases, a review of the linkages. WHO Special Topics 3, 2013.
(20) Pereira, P. C.; Navarro, E. C. J. *J. Venomous Anim. Toxins Incl. Trop. Dis.* **2013**, *19*, 19−34.
(21) Santos, M. F. C.; Harper, P. M.; Williams, D. E.; Mesquita, J. T.; Pinto, E. G.; Costa-Silva, T. A.; Hajdu, E.; Ferreira, A. G.; Santos, R. A.; Murphy, P. J.; Andersen, R. J.; Tempone, A. G.; Berlinck, R. G. S. *J. Nat. Prod.* **2015**, *78*, 1101−1112.
(22) Reimão, J. Q.; Migotto, A. E.; Kossuga, M. H.; Berlinck, R. G. S.; Tempone, A. G. *Parasitol. Res.* **2008**, *103*, 1445−1450.
(23) Kossuga, M. H.; Nascimento, A. M.; Reimão, J. Q.; Tempone, A. G.; Taniwaki, N. N.; Veloso, K.; Ferreira, A. G.; Cavalcanti, B. C.; Pessoa, C.; Moraes, M. O.; Mayer, A. M. S.; Hajdu, E.; Berlinck, R. G. S. *J. Nat. Prod.* **2008**, *71*, 334−339.
(24) Gray, C. A.; de Lira, S. P.; Silva, M.; Pimenta, E. F.; Thiemann, O. H.; Oliva, G.; Hajdu, E.; Andersen, R. J.; Berlinck, R. G. S. *J. Org. Chem.* **2006**, *71*, 8685−8690.
(25) Somsák, L.; Kovács, L.; Tóth, M.; Ösz, E.; Szilágyi, L.; Györgydeák, Z.; Dinya, Z.; Docsa, T.; Tóth, B.; Gergely, P. J. *J. Med. Chem.* **2001**, *44*, 2843−2848.
(26) Czifrák, K.; Somsák, L. *Tetrahedron Lett.* **2002**, *43*, 8849−8852.
(27) Czifrák, K.; Szilágyi, P.; Somsák, L. *Tetrahedron: Asymmetry* **2005**, *16*, 127−141.
(28) Czifrák, K.; Gyóllai, V.; Kövér, K. E.; Somsák, L. *Carbohydr. Res.* **2011**, *346*, 2104−2112.
(29) Hanington, P. M.; Jung, M. E. *Tetrahedron Lett.* **1994**, *35*, 5145−5148.
(30) Somsák, L.; Nagy, V. *Tetrahedron: Asymmetry* **2000**, *11*, 1719−1727.
(31) Barrow, R. A.; Capon, R. *Nat. Prod. Lett.* **1993**, *1*, 243−250.
(32) Gribble, G. W. *Fortschr. Chem. Org. Naturst.* **2010**, *91*, 1−505.
(33) Andersen, R. J.; Wolfe, M. S.; Faulkner, D. J. *Mar. Biol.* **1974**, *27*, 281−285.
(34) Wischang, D.; Hartung, J. *Tetrahedron* **2011**, *67*, 4048−4054.
(35) Wischang, D.; Radlow, M.; Schulz, H.; Vilter, H.; Viehweger, L.; Altmeyer, M. O.; Kegler, C.; Herrmann, J.; Müller, R.; Gaillard, F.; Delage, L.; Leblanc, C.; Hartung, J. *Bioorg. Chem.* **2012**, *44*, 25−34.
(36) Wischang, D.; Radlow, M.; Hartung, J. *Dalton Trans.* **2013**, *42*, 11926−11940.
(37) Rua, C. P. J.; Oliveira, L.; Froes, A.; Tschoeke, D. A.; Soares, A. C.; Leomil, L.; Gregoracci, G. B.; Hajdu, E.; Thompson, C. C.; Berlinck, R. G. S.; Thompson, F. L., submitted 2017.
(38) Bailey, D. M.; Johnson, R. E. *J. Med. Chem.* **1973**, *16*, 1300−1302.
(39) Ye, C.; Shreeve, J. M. *J. Org. Chem.* **2004**, *24*, 8561−8563.
(40) Troegel, B.; Lindel, T. *Org. Lett.* **2012**, *14*, 468−471.
(41) Berman, J. J. *Taxonomic Guide to Infectious Diseases: Understanding the Biologic Classes of Pathogenic Organisms*; Academic Press: Amsterdam, 2012; pp 95−98.
(42) Bazzini, P.; Wermuth, C. G. In *The Practice of Medicinal Chemistry*, 4th ed.; Wermuth, C. G.; Aldous, D.; Raboisson, P.; Rognan, D., Eds.; Elsevier: Amsterdam, 2015; p 338.
(43) Bazzini, P.; Wermuth, C. G. In *The Practice of Medicinal Chemistry*, 4th ed.; Wermuth, C. G.; Aldous, D.; Raboisson, P.; Rognan, D., Eds.; Elsevier: Amsterdam, 2015; p 341.
(44) Wells, T. N.; Hooft van Huijsduijnen, R.; Van Voorhis, W. C. *Nat. Rev. Drug Discovery* **2015**, *6*, 424−442.
(45) Scala, F.; Fattorusso, E.; Menna, M.; Taglialatela-Scafati, O.; Tierney, M.; Kaiser, M.; Tasdemir, D. *Mar. Drugs* **2010**, *8*, 2162−2174.
(46) Tasdemir, D.; Topaloglu, B.; Perozzo, R.; Brun, R.; O'Neill, R.; Carballeira, N. M.; Zhang, X.; Tonge, P. J.; Linden, A.; Ruedi, P. *Bioorg. Med. Chem.* **2007**, *15*, 6834−6845.
(47) Miguel, D. C.; Flannery, A. R.; Mittra, B.; Andrews, N. W. *Infect. Immun.* **2013**, *81*, 3620−3626.
(48) Peloso, E. F.; Dias, L.; Queiroz, R. M.; Leme, A. F.; Pereira, C. N.; Carnielli, C. M.; Werneck, C. C.; Sousa, M. V.; Ricart, C. A.; Gadelha, F. R. *Biochim. Biophys. Acta, Proteins Proteomics* **2016**, *1*, 1−10.
(49) Miguel, D. C.; Yokoyama-Yasunaka, J. K.; Andreoli, W. K.; Mortara, R. A.; Uliana, S. R. *J. Antimicrob. Chemother.* **2007**, *3*, 526−34.
(50) Trager, W.; Jensen, J. B. *Science* **1976**, *193*, 673−675.
(51) Lambros, C.; Vanderberg, J. P. *J. Parasitol.* **1979**, *65*, 418−420.
(52) Smilkstein, M.; Sriwilaijaroen, N.; Kelly, J. X.; Wilairat, P.; Riscoe, M. *Antimicrob. Agents Chemother.* **2004**, *48*, 1803−18063.
(53) Denizot, F.; Lang, R. *J. Immunol. Methods* **1986**, *89*, 271−277.
(54) Gorka, A. P.; Jacobs, L. M.; Roepe, P. D. *Malar. J.* **2013**, *12*, 332.

DOI: 10.1021/acs.jnatprod.7b00876
J. Nat. Prod. XXXX, XXX, XXX−XXX